nature cell biology

Haemocytes control stem cell activity in the *Drosophila* intestine

Arshad Ayyaz[1], Hongjie Li[1,2] and Heinrich Jasper[1,3]

Coordination of stem cell activity with inflammatory responses is critical for regeneration and homeostasis of barrier epithelia. The temporal sequence of cell interactions during injury-induced regeneration is only beginning to be understood. Here we show that intestinal stem cells (ISCs) are regulated by macrophage-like haemocytes during the early phase of regenerative responses of the *Drosophila* intestinal epithelium. On tissue damage, haemocytes are recruited to the intestine and secrete the BMP homologue DPP, inducing ISC proliferation by activating the type I receptor Saxophone and the Smad homologue SMOX. Activated ISCs then switch their response to DPP by inducing expression of Thickveins, a second type I receptor that has previously been shown to re-establish ISC quiescence by activating MAD. The interaction between haemocytes and ISCs promotes infection resistance, but also contributes to the development of intestinal dysplasia in ageing flies. We propose that similar interactions influence pathologies such as inflammatory bowel disease and colorectal cancer in humans.

The intestinal epithelium constitutes a regenerative, permeable barrier that interacts with commensal and pathogenic microbes and responds to environmental toxins and to physical stress while allowing selective nutrient resorption[1–4]. To maintain homeostasis, it is critical that regenerative activity is precisely coordinated with innate immune responses. How this coordination is achieved, however, remains unclear. The *Drosophila* intestinal epithelium is a powerful model to study epithelial immunity, damage responses and regeneration[5]. It mounts innate immune responses to control commensal and pathogenic microorganisms and is regenerated by a population of ISCs that give rise to both enterocytes (ECs) and enteroendocrine cells[2,5–8].

ISCs exhibit strong proliferative plasticity in the wake of damaging environmental challenges[5,9]. Regenerative responses are controlled by local and paracrine signals, derived either from damaged ECs or from the surrounding visceral muscle, that activate a host of pro-proliferative signalling pathways in ISCs (refs 5,9). EC-derived interleukin 6-like cytokines called Unpaireds (UPD1-3) promote ISC proliferation either directly by activating JAK/STAT signalling in ISCs, or indirectly by inducing expression of EGF Receptor (EGFR) ligands, such as *vein*, in the visceral muscle, which then activate EGFR signalling in ISCs (refs 9–16). Proliferative activity of ISCs is further controlled by Wingless signalling, Jun-N-terminal Kinase, and insulin signalling, among other signals[2,9,17].

The BMP homologue Decapentaplegic (DPP) plays recurrent and complex roles in the regulation of ISCs (refs 18–22). Under homeostatic conditions, DPP signalling is required for the differentiation of acid-secreting Copper cells in the middle midgut region[18,20], and in response to tissue damage, DPP secreted from visceral muscle engages the type I receptor Thickveins (TKV) and the *Drosophila* Smad protein MAD to promote ISC return to quiescence[20]. In contrast, a second BMP type I receptor, Saxophone (SAX), is required to induce proliferation[21]. The relationship between TKV and SAX-mediated regulation of ISC proliferation remains unclear, as does the relevant source of DPP (refs 19–22).

Work in vertebrates has implicated immune cells in the induction of mitotic activity and regeneration in intestinal epithelia[23–25]. In *Drosophila*, macrophage-like haemocytes constitute a major population of blood cells[26] that mediate infection responses and tissue repair[27], yet if and how these cells influence regeneration in the intestinal epithelium has not been addressed.

Here, we identify a role for DPP derived from gut-associated haemocytes in the regulation of ISC proliferation. We find that DPP secreted from these haemocytes induces ISC proliferation through SAX-mediated activation of Smad on X (SMOX) in the initial response to *Erwinia carotovora carotovora* 15 (*Ecc*15; ref. 13). In the later phase of the regenerative response, ISCs express TKV, diverting the DPP signal from SAX/SMOX to MAD, restoring ISC quiescence. Differential expression of SAX and TKV thus allows selective responses of ISCs to DPP at different time points during a regenerative episode. The regulation of ISC proliferation by haemocyte-derived DPP is critical for host

[1]Buck Institute for Research on Aging, 8001 Redwood Boulevard, Novato, California 94945-1400, USA. [2]Department of Biology, University of Rochester, River Campus Box 270211, Rochester, New York 14627, USA.
[3]Correspondence should be addressed to H.J. (e-mail: hjasper@buckinstitute.org)

Received 16 October 2014; accepted 7 April 2015; published online 25 May 2015; DOI: 10.1038/ncb3174

survival during acute intestinal infection, but it also contributes to the development of intestinal dysplasia and the loss of intestinal barrier function in ageing flies. Our findings have important implications for our understanding of regenerative processes in barrier epithelia.

RESULTS

Gut-associated haemocytes are required to induce ISC proliferation

To examine whether intestinal regeneration in flies is influenced by haemocytes, we expressed pro-apoptotic genes (*head involution defective*, *hid*, or *reaper*, *rpr*) in developing haemocytes at mid-larval stages, using Gal4 driven by the *Hml*Δ promoter (Supplementary Fig. 1A,B). *Hml*Δ is active in larval and adult haemocytes[28] and in motile extra-epithelial phagocytic cells in the proventriculus and the hindgut[29], but is not expressed in the intestinal epithelium (Supplementary Fig. 1C) or other adult tissues (Supplementary Fig. 1D,E). The resulting 'haemoless' flies emerge as widely normal adults and are viable and reproductively competent, but are sensitive to systemic infection[28] (Supplementary Fig. 1B,F). At young ages, the size, structure and cellular composition of the intestinal epithelium of these animals are indistinguishable from wild-type (Supplementary Fig. 1G,H). However, the mitotic response of ISCs to acute intestinal damage by oxidative stress (induced by Paraquat) or infection (by the enteropathogens *Ecc*15 (refs 13,15) or *Pseudomonas entomophila*[10] (*PE*)) is impaired (Fig. 1a–c: ISCs are the only dividing cells in the intestinal epithelium, quantification of phospho-Histone H3-positive cells is thus commonly used to assess ISC proliferation; the number of DELTA+ ISCs remains unchanged; Supplementary Fig. 1I). The same effect is observed when haemocytes are ablated specifically in adults (Supplementary Fig. 2A).

We examined whether haemocytes interact with the intestinal epithelium, and found haemocytes in the abdominal cavity concentrated in large unstructured aggregates, located within the folds of the midgut (Fig. 1d,e,i). Occasionally, individual haemocytes are also seen attached to the intestinal epithelium (Fig. 1f,g). Gut-associated immune cells express various haemocyte-specific markers such as EATER and Nimrod (NIMC1), which identify plasmatocytes, phagocytic cells with similarity to mammalian monocytes and macrophages[30,31] (Fig. 1f). These cells are closely associated with the intestinal basement membrane (visualized using the basement membrane-specific type IV collagen encoded by *Viking*[11,32]; Fig. 1g,h).

On oral infection with *PE* or *Ecc*15, haemocytes (expressing GFP under the control of the *Hml*Δ (ref. 33) or DsRed under the control of the *eater* promoter[30]) are increasingly found attached to the visceral muscle surrounding the intestinal epithelium throughout the midgut (Fig. 2a–d and Supplementary Figs 2B,C and 8A; also refer to Figs 1i and 2b and Supplementary Fig. 3G for identification of arbitrarily assigned morphologically distinguishable midgut regions). Infection also leads to a significant increase in the size of haemocyte clumps located in folds of the middle and posterior midgut (PM; Fig. 2a,b and Supplementary Fig. 2B). This increased association of haemocytes with the gut is transient, as 24 h after an infection the number of haemocytes attached to the intestine declines (Fig. 2e). We used mosaic analysis with a repressible cell marker[34] (MARCM) to examine whether the increased numbers of gut-associated haemocytes result from a proliferative response of haemocytes, but did not find any *eater*::DsRed+ haemocytes that expressed GFP (as would be expected if mitotic haemocytes or precursors would generate MARCM clones) in any tissue during or after *Ecc*15 challenge (Supplementary Fig. 2E,F). Instead, single haemocytes isolated from haemolymph of *Ecc*15-challenged flies were bigger in size and more oval in shape than haemocytes from controls, suggesting that circulating haemocytes are activated and change their morphology during intestinal stress (Supplementary Fig. 2D).

Haemocyte-derived DPP is required for ISC proliferative response

As these data suggested that local or paracrine signals from haemocytes might modulate ISC function, we performed an RNA-mediated interference (RNAi) screen targeting putative secreted factors in haemocytes, and identified DPP as required in haemocytes to induce ISC proliferation on oxidative stress (Fig. 3a and Supplementary Fig. 3A) and pathogen exposure (Fig. 3b,c). Knockdown of *dpp* in only adult haemocytes (using either a temperature-sensitive combination of *Hml*Δ*::Gal4* with *tub::Gal80*^{ts}, or an RU486-inducible system based on the same promoter, *Hml*Δ*::GS*) was sufficient to limit ISC responses (Fig. 3a–c and Supplementary Fig. 3B). *Hml*Δ*::GS* recapitulates the expression profile of *Hml*Δ*::Gal4* in larvae and adults (Supplementary Fig. 3F). Knockdown of *dpp* was also sufficient to inhibit ISC responses to *Ecc*15 infection when driven by a separate haemocyte driver, *He*::Gal4 (ref. 35), but not when driven by either a hindgut driver (*byn*::Gal4) or a proventriculus driver (*cardia*::Gal4), confirming that the loss of ISC proliferation in *Hml*::Gal4, UAS::*dpp*^{RNAi} flies is due to knockdown of DPP specifically in haemocytes and not due to unspecific knockdown in intestinal cells (Supplementary Fig. 3C). Accordingly, knockdown of *dpp* in ECs (NP1::Gal4), ISCs and enteroblasts (EBs) (*esg*::Gal4), trachea (*btl*::Gal4), or visceral muscle (*how*::Gal4) did not impact ISC responses to Paraquat (Supplementary Fig. 3D). The two *dpp*^{RNAi} lines used in these analyses efficiently reduce *dpp* messenger RNA levels in haemocytes or visceral muscle when knocked down using *Hml*Δ::Gal4 or *how*::Gal4, respectively (Supplementary Fig. 3E).

We did not observe any differences in number and distribution of DPP-deficient haemocytes compared to wild-type flies (Supplementary Fig. 3G). Furthermore, haemocyte-derived DPP-deficient (HDD) flies are immune-competent to systemic *PE* infection and recruitment of haemocytes to the intestinal epithelium was still observed in HDD flies (Supplementary Figs 1F and 3H).

DPP is expressed in haemocytes of adult flies, is induced in response to infection, and can modulate the innate immune response[36]. Recapitulating these observations, we found that Paraquat exposure or *Ecc*15 infection induced *dpp* in haemocytes (Supplementary Fig. 3I,J). To assess whether haemocyte-derived DPP signals directly to ISCs, we monitored a DPP–GFP fusion protein[37] expressed specifically in haemocytes (using *Hml*Δ::GS and *Hml*Δ::Gal4). DPP–GFP secreted by gut-associated haemocytes is detected on the intestinal surface (Fig. 3d). DPP–GFP (but not GFP when expressed alone from *Hml*Δ::Gal4) was also detected within the gut epithelium on diploid progenitor cell nests (basally located cells with strong Armadillo expression, representing doublets of ISCs and EBs; Fig. 3e). Following *Ecc*15 challenge, accumulation of haemocyte-secreted DPP–GFP was observed at the basement

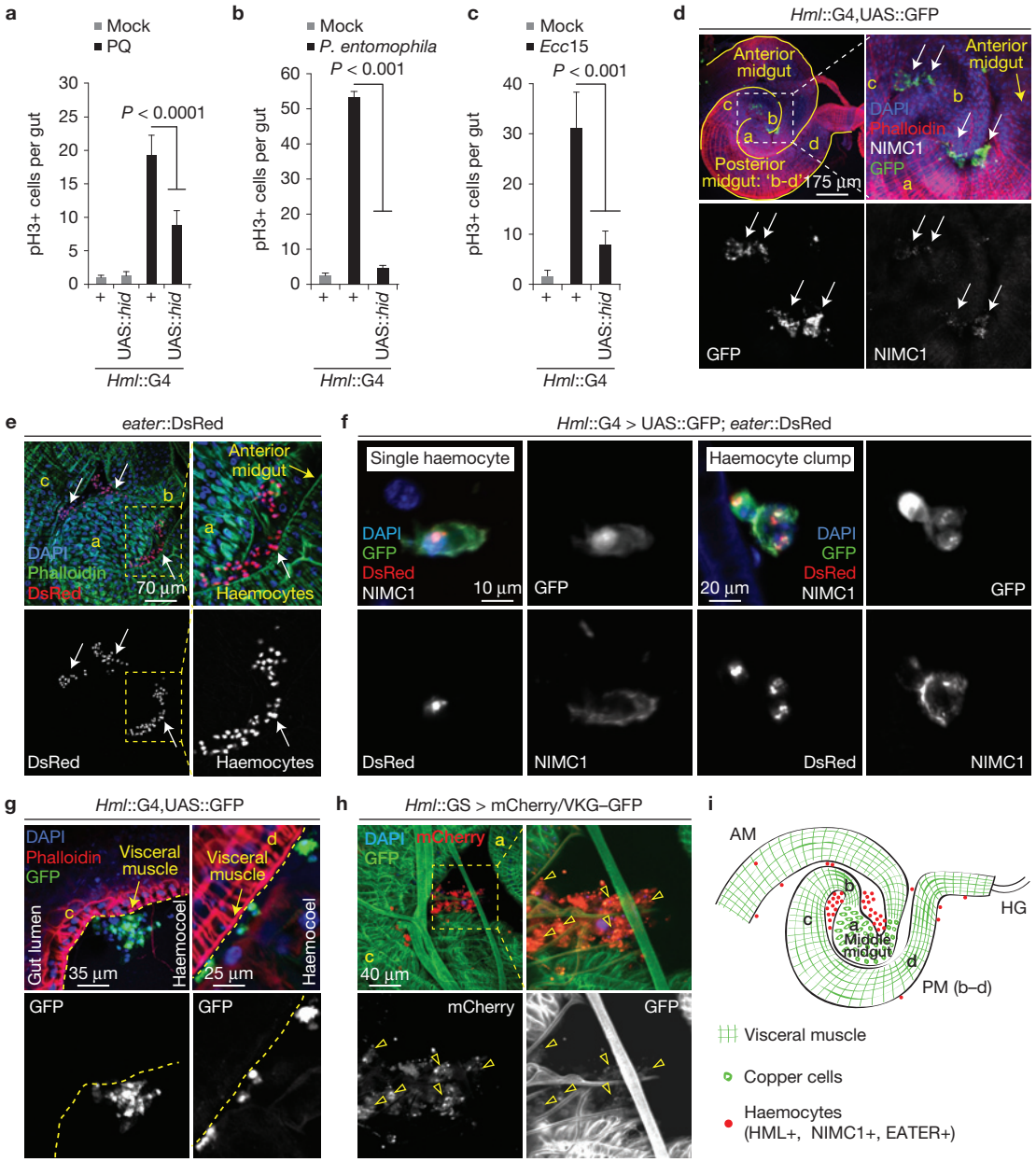

Figure 1 Gut-associated haemocytes are required for ISC proliferation. (**a**–**c**) Mitotic activity of ISCs (identified by phospho-Histone H3-positive cells) in intestines of 3-day-old haemoless flies exposed to Paraquat (PQ; **a**), *PE* (**b**) or *Ecc*15 (**c**), compared with wild-type controls. (**d**,**e**) Haemocytes associated with the fly gut under normal rearing conditions can be detected using multiple haemocyte markers: *Hml*Δ::Gal4 driver and NIMC1 (**d**; white arrows) or *eater*::DsRed reporter (**e**; white arrows), and arbitrary midgut regions are identified morphologically using phalloidin staining that marks Actin (**d**,**e**; also see Supplementary Fig. 2G). (**f**) Haemocytes attach to fly intestine as single cells or clumps of irregular shape and express all three haemocyte markers: *Hml* (haemolectin), *eater* and NIMC1 (Nimrod). Note that the haemocyte reporter nuclear *eater*::DsRed provides efficient quantification for the actual number of haemocytes per clump. (**g**) Single haemocytes or clumps attach midgut at the outer surface of visceral muscle (marked by phalloidin staining; yellow arrows); where c and d refer to posterior midgut regions c and d. (**h**) Type IV collagen encoded by Viking (detected as a fused protein with GFP) appears associated with gut-associated haemocytes (arrowheads) at region c of the posterior midgut; 'a' indicates the middle midgut region. (**i**) Cartoon showing morphological features of arbitrarily assigned midgut regions (also see Supplementary Fig. 2G) where haemocytes usually attach to the fly intestine under homeostatic conditions. HML: Haemolectin, NIMC1: Nimrod, AM: anterior midgut, PM (b–c): posterior midgut regions b–c, HG: hindgut; and 'a' identifies middle midgut containing large Copper Cells. Error bars indicate s.e.m. (**a**–**c**: $n=12$ flies from a representative of 3 independent experiments), *P* values from Student's *t*-test. One representative image from 15 flies tested in a single experiment, which was repeated 3 times, is shown in **d**–**h**.

membrane, specifically close to DELTA+ cells in the intestinal epithelium, suggesting that haemocyte-secreted DPP can penetrate the visceral muscle layer to bind to ISCs (Fig. 3f and Supplementary Fig. 3K).

Haemocyte-derived DPP maintains basal stem cell activity

We investigated whether DPP from haemocytes might not only influence acute infection responses, but also modulate basal ISC activity. We used a split-lacZ reconstitution assay to label selected

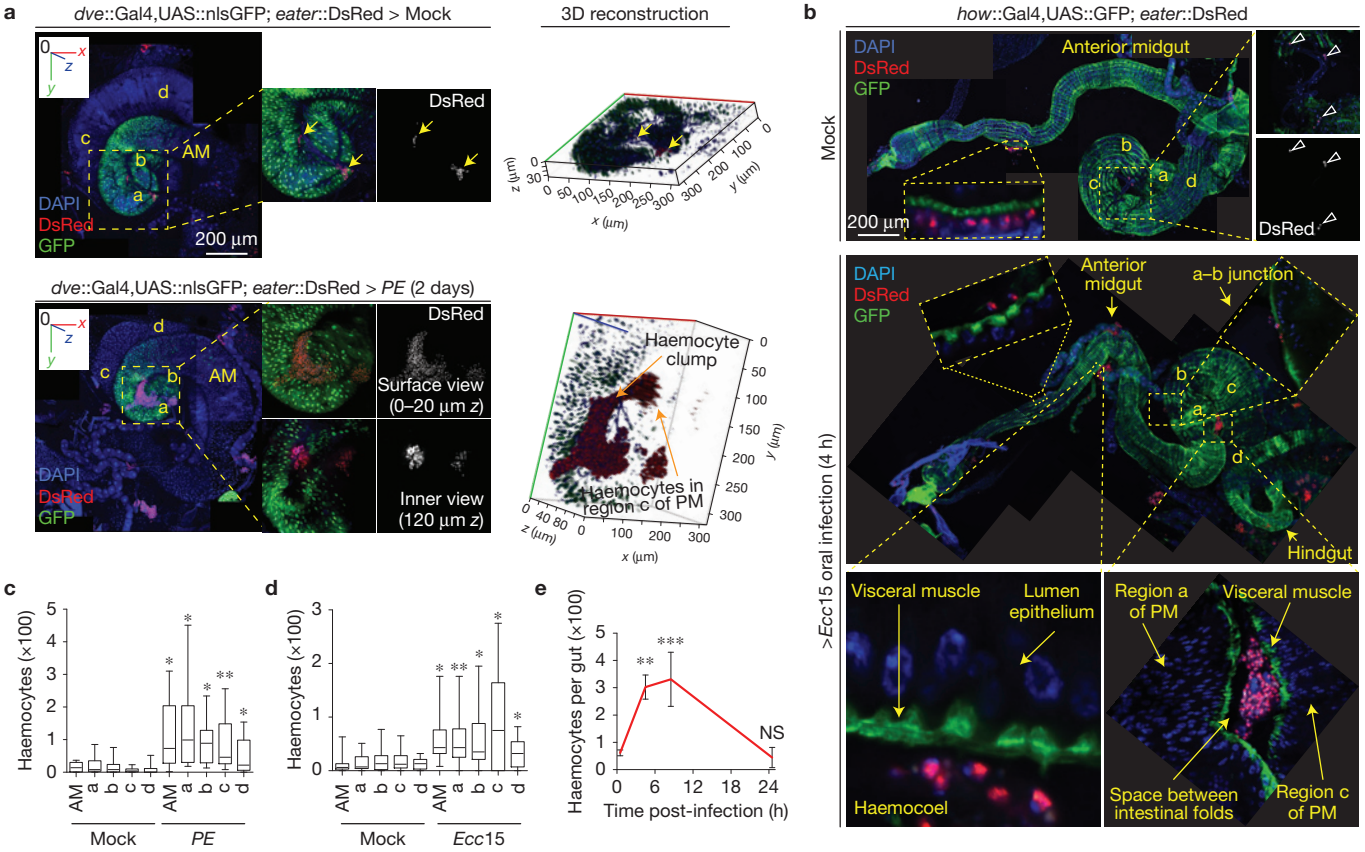

Figure 2 Haemocytes dynamically recruit to the gut during stress. (**a**) Large haemocyte clumps are observed associated with an un-stretched *PE*-infected, but not mock-treated, intestine (also see Supplementary Fig. 2G for *dve*::Gal4 expression pattern in midgut regions). Three-dimensional images are generated using a Zeiss LSM700 confocal microscope platform (zeiss.com) to show the extent of penetration of haemocyte clumps into midgut folds. AM: anterior midgut, a: middle midgut, and b–d: posterior midgut regions b–d. (**b**) Haemocyte recruitment along the anterior-to-posterior axis in partially stretched guts is shown after mock treatment or 4 h of *Ecc*15 challenge. Note that *eater*::DsRed+ haemocytes either attach to the external surface of the intestine or appear trapped within midgut folds (see fold between regions a and c) or can be occasionally detected penetrating the visceral muscle layer (see a–b junction) in *Ecc*15-infected flies. (**c**,**d**) *eater*::DsRed+ haemocytes found in the vicinity of different regions of un-stretched midguts following oral challenge with *PE* (**c**; 2 days after infection) or *Ecc*15 (**d**; 4 h after infection) are quantified and compared with those under mock-treated conditions. Note that these quantitative studies on region-specific haemocyte recruitment are performed on un-stretched intestines, as stretching of the gastrointestinal tube along the anterior-to-posterior axis results in dissociation of haemocytes recruited to the midgut folds (also see **b**). (**e**) Quantification of total *eater*::DsRed+ haemocytes recruited per midgut during the course of an *Ecc*15-infection episode of 24 h. Error bars indicate range (**c**: $n=22$ and **d**: $n=15$ flies; where boxes show 25–75% percentile and the horizontal bar within each box is the population median) or s.e.m. (**e**: $n=15$ flies) from a representative of 3 experiments, *P* values from Student's *t*-test. One representative image from 15 flies tested in a single experiment (replicated 3 times) is shown in **a** and **b**. NS: not significant, $^{*}P<0.05$, $^{**}P<0.01$, $^{**}P<0.001$.

ISCs heritably[38], and found that haemocyte-derived DPP is required for induction (clone numbers per gut) and growth (cells per clone) of ISC-derived cell clones (Fig. 3g,h,j and Supplementary Fig. 3L). We did not observe signs of apoptosis (using Apoliner[39]) in flies that co-express dpp^{RNAi} directly under the control of the *Hml*Δ promoter (*Hml*Δ::dpp^{RNAi}), confirming that the reduced clone size in HDD flies is due to decreased ISC proliferation (Supplementary Fig. 3M).

Haemocyte transplantation rescues ISC proliferation in haemoless and HDD flies

When wild-type or DPP-overexpressing haemocytes were transplanted into haemoless flies at 12 days of age, the proliferative response of ISCs to Paraquat treatment and *Ecc*15 infection, as well as clone growth recovered (Fig. 3i,j; we used 12-day-old flies as donors, as we found that a substantial number of haemocytes could only be transferred when donor flies were older than 3 days, Supplementary Fig. 3N; transplanted haemocytes associated with the intestine, Supplementary Fig. 3O). Reduced ISC proliferation in haemoless or HDD flies is thus not caused by unspecific or unidentified defects, but by the lack of haemocyte-derived factors. Accordingly, transplantation of DPP-deficient haemocytes (from donors expressing dpp^{RNAi} under the control of *Hml*Δ::*Gal4*) failed to rescue ISC proliferation in haemoless flies (Fig. 3i,j).

Haemocyte-derived DPP acts in parallel to JAK/STAT and EGFR pathways

The positive role of haemocyte-derived DPP in regulating ISC proliferation is in contrast to the established inhibition of ISC proliferation by TKV and MAD[20,22]. To explain this paradox, we sought to temporally resolve the response of ISCs to DPP signalling. ISCs respond to *Ecc*15

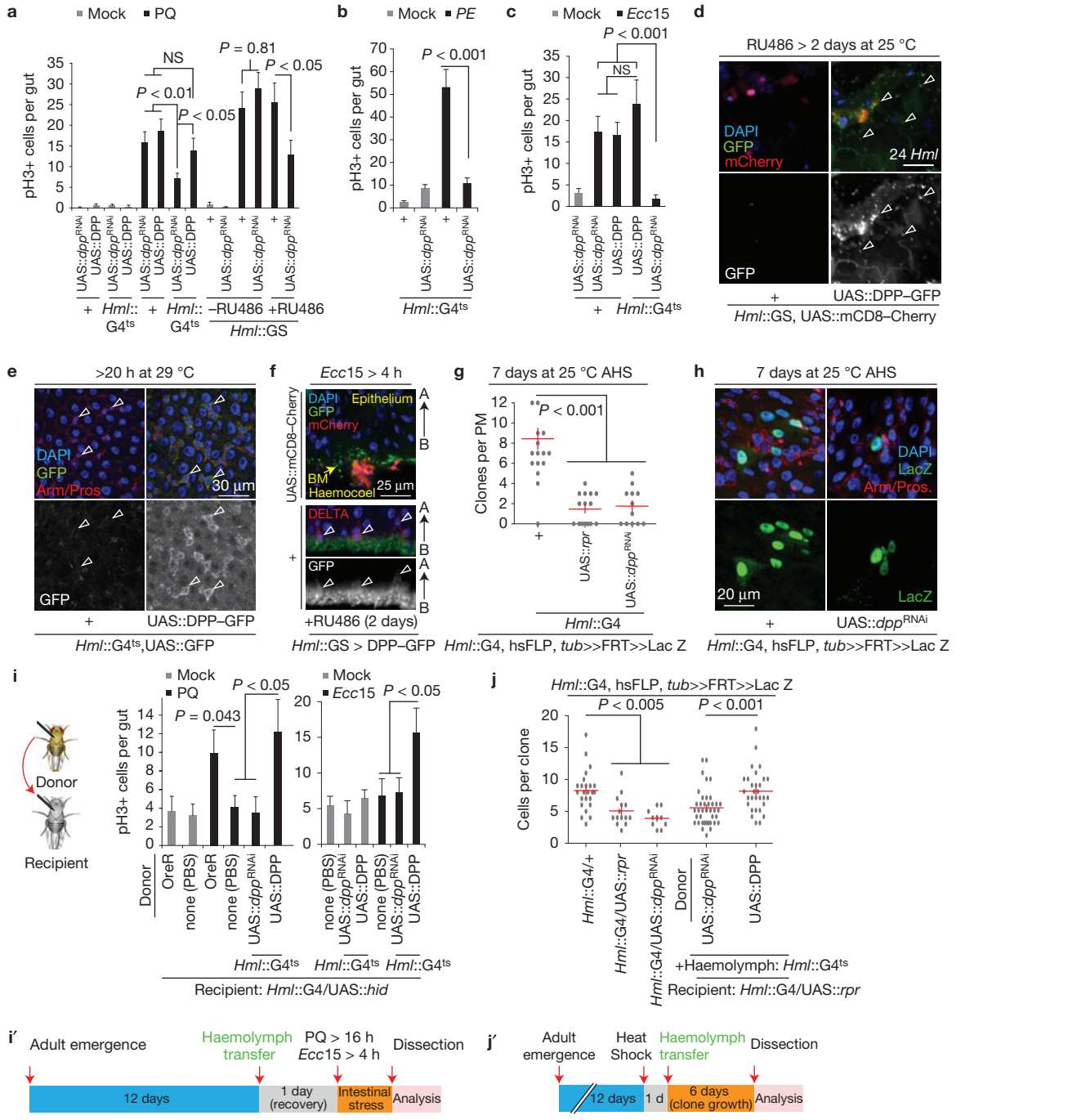

Figure 3 Haemocyte-derived DPP acts on ISCs to promote proliferation. (**a**–**c**) ISC proliferation induced by Paraquat (PQ) treatment (**a**) or bacterial infection (**b**,**c**) is significantly reduced when *dpp* is knocked down specifically in adult haemocytes either using *Hml*Δ::Gal4 combined with *tub*::Gal80^{ts} (*Hml*::G4^{ts}) (**a**–**c**) or mifepristone (RU486)-sensitive *Hml*::GS (**a**) and a *dpp*^{RNAi} line (Bloomington Stock no. 33618). Acute DPP overexpression in haemocytes neither induces ISC proliferation in the absence of stress (**a**) nor enhances ISC mitotic activity during tissue damage (**a**,**c**). (**d**,**e**) DPP–GFP fusion protein expressed in adult haemocytes is detected (using anti-GFP antibody; see Methods) on the intestinal surface (**d**: arrowheads) and on ISC/EB doublets identified by their basal location and strong Armadillo expression (**e**: arrowheads). (**f**) During *Ecc*15 challenge, DPP–GFP fusion protein expressed in haemocytes can be seen accumulated at the basal membrane (BM) with specific binding to DELTA+ ISCs. (**g**–**j**) Lineage tracing from ISCs using FRT recombination of a split α-*tubulin*–lacZ transgene shows reduced clone number (**g**) and clone size (**h**) in haemoless and HDD animals. This defect in clone formation and reduced ISC proliferative response observed in haemoless flies following PQ treatment or *Ecc*15 infection is rescued on haemolymph transfer from wild-type flies (**i**) or from flies overexpressing DPP specifically in haemocytes, but not on transfer of *dpp*^{RNAi}-expressing haemocytes (**i**,**j**), and the experimental timeline is shown in **i**′ and **j**′. AHS: after heat shock. Error bars indicate s.e.m. (**a**–**c**: $n = 10$; **g**: $n = 12$; **i** (for PQ treatment): Mock: OreR, $n = 17$; none(PBS), $n = 16$; and PQ: OreR, $n = 17$; none(PBS), $n = 36$; UAS::*dpp*^{RNAi}, $n = 13$; UAS::DPP, $n = 16$; **i** (for *Ecc*15 treatment): Mock and *Ecc*15: $n = 10$; **j**: $n = 9$ flies; sufficient sample sizes for pH3 analyses in fly gut[11,13]), *P* values from Student's *t*-test. Data shown in **a**–**c**, **g** and **j** are representative of 3 independently performed experiments, and those shown in **i** are a composite from 2 separate experiments. One representative image from 9 flies tested in a single experiment (repeated 3 times independently) is shown in **d**–**f** and **h**.

infection by an early burst of proliferative activity ('induction phase': 4 to 12 h post-infection) followed by a return to quiescence when the infection is resolved ('recovery phase': 16 to 24 h post-infection)[13] (Fig. 4a). Haemoless and HDD flies showed a significantly reduced proliferative response in the inductive phase (Fig. 4a).

The activation of JAK/STAT and EGFR pathways in guts of infected haemoless and HDD flies is normal (Supplementary Fig. 4A-C), suggesting that DPP from haemocytes is required for ISC proliferation in parallel to the JAK/STAT/EGFR signal. Accordingly, knockdown of haemocyte-derived *dpp* also limits the induction of ISC proliferation by UPD2 overexpression in ECs (Supplementary Fig. 4D), and acute overexpression of DPP in haemocytes or in visceral muscle is not sufficient to induce ISC proliferation in the absence of injury (Supplementary Fig. 4E) nor shows an additive effect on ISC activity on tissue damage (Fig. 3a,c). Long-term DPP overexpression in haemocytes, however, increases proliferation of ISCs both in the anterior and posterior midgut (Supplementary Fig. 4F). ISCs thus integrate signals from haemocyte-derived DPP and EC/muscle-derived UPD/VEIN ligands, and require inputs from all three pathways to achieve appropriate proliferative responses to damage. No differences in feeding were observed between wild-type, haemoless and HDD flies, with or without infection (Supplementary Fig. 4G,H).

Activation of DPP signalling in ISCs during inductive phase

To assess whether haemocyte-derived DPP would influence DPP signalling directly in ISCs, we used the DPP pathway activity reporter *Dad*::nlsGFP (ref. 40). Under basal conditions, this reporter describes two opposing DPP signalling gradients in the posterior midgut[18], with high activity in the distal borders to the gastric region and the hindgut (regions b and d in Fig. 4b), and weak reporter activity in the central region 'c' (Fig. 4b)[18]. Although haemocyte-derived DPP induces ISC proliferation throughout the anterior and posterior midgut (Supplementary Fig. 4F and Supplementary Fig. 5A), we focused our further observations on region c of the posterior midgut because of the high concentration of haemocytes present (Fig. 1d,e,h,i and Fig. 2b,d) and the low levels of basal *Dad*::nlsGFP in this region (Fig. 4b). During the inductive phase after challenge with *Ecc*15, *Dad*::nlsGFP activity increases in region c (in both diploid and polyploid cells, including DELTA-positive ISCs) in wild-type flies as early as 4 h after challenge (AC; Fig. 4c–e). This induction was absent in haemoless and HDD flies, and could be restored by haemolymph transfer from wild-type animals (Fig. 4c–e). Later induction of DPP signalling activity in this region (12–16 h AC), however, was not affected (Fig. 4c), suggesting that secretion of DPP from the visceral muscle, which is observed at 24 h after challenge[20] (Supplementary Fig. 5B), is not influenced by haemocytes.

Nuclear translocation of SMOX requires haemocyte-derived DPP

DPP signals through TKV to phosphorylate MAD[41]. Unexpectedly, MAD phosphorylation (pMAD) was not observed in ISCs in region c of wild-type flies at 4 h AC (Supplementary Fig. 5C), a stage where ISCs are mitotically active (Fig. 4a), but was high in ISCs at 16 h AC, ruling out a role for MAD activity in the induction of proliferation, and suggesting that phosphorylation of MAD might be limited to the recovery period to promote return of ISCs to a quiescent state (consistent with ref. 20). We therefore tested whether another MAD-like nuclear factor, SMOX (also known as dSMAD2; ref. 42), may act to regulate the proliferative response of ISCs. A genomic rescue construct encoding a SMOX–FLAG fusion protein[43] shows high expression specifically in ISCs and EBs of the PM (Fig. 5a). SMOX–FLAG is localized in the cytoplasm of these cells under homeostatic conditions, yet after 4 h of *Ecc*15 infection, nuclear translocation of SMOX is observed, and this translocation is dependent on haemocyte-derived DPP (Fig. 5a,b). Consistent with these observations, knockdown of *Smox* in ISCs prevents induction of *Dad*::nlsGFP specifically in DELTA+ ISCs, but not in other cells, in region c of the PM at 4 h after *Ecc*15 challenge, indicating that *Dad* is a transcriptional target of SMOX in ISCs (Supplementary Fig. 5E).

Regulation of SMOX activity by haemocyte-derived DPP in ISCs thus precedes the increase in MAD phosphorylation during an infection, suggesting that SMOX may mediate the pro-proliferative effects of haemocyte-derived DPP. dActivin and Dawdle, TGFβ BMP family ligands that have been implicated in SMOX regulation in other contexts[44,45], are not likely to be required for SMOX activation in ISCs, because ubiquitous knockdown of these ligands does not inhibit infection-induced proliferation (Supplementary Fig. 5D).

TKV/MAD signalling antagonizes ISC activity induced on SAX/SMOX pathway stimulation

To gain insight into the selective activation of SMOX and MAD by DPP after an infection, we explored the role of individual type I receptors. SMOX is engaged by the type I receptor Saxophone, and we found indeed that SAX is required for SMOX nuclear translocation after *Ecc*15 treatment (Fig. 5a,b). SAX can be activated both by DPP (ref. 46) and Glass Bottom Boat[47] (GBB). Consistent with recent reports, we detected a strong reduction in mitotic activity of ISCs at the 'inductive' phase of *Ecc*15 infection when *gbb* was knocked down specifically in ECs, but not in haemocytes, suggesting that both DPP and GBB are required for ISC proliferation. However, the functional source for these ligands is different: haemocytes for DPP and ECs for GBB (refs 21,22; Supplementary Fig. 6A).

On binding to DPP, SAX plays a complex role in regulating MAD activity in conjunction with TKV (ref. 46). To dissect the relative contributions of SAX/SMOX and TKV/MAD signalling in the control of ISC proliferation, we knocked down *sax* and SMOX, as well as TKV and MAD, specifically in ISCs, and triggered regeneration by exposure to bacteria. *sax*/SMOX knockdown prevented induction of proliferation, and TKV/MAD knockdown did not impact the inductive phase, but prevented recovery into quiescence (Fig. 5c). These pathways do not seem to crosstalk in ISCs, as Tkv is required and sufficient to phosphorylate MAD in ISCs, and SAX is not (Supplementary Fig. 6B,C).

These results provided a model for the dual role of DPP in the regenerative response: initial engagement of SAX/SMOX signalling by haemocyte-derived DPP results in induction of ISC proliferation, and activation of TKV/MAD signalling by muscle-derived DPP (which is induced at later stages) directs recovery to the quiescent state (as previously described in ref. 20). To test this model, we performed lineage tracing and epistasis analysis. We used MARCM (ref. 34) to trace lineages of ISCs mutant for various DPP signalling components: *sax* and *Smox* mutant ISCs generated smaller MARCM clones than wild-type controls (Fig. 5d and Supplementary Fig. 6D), confirming that the basal activity of SAX/SMOX signalling is required

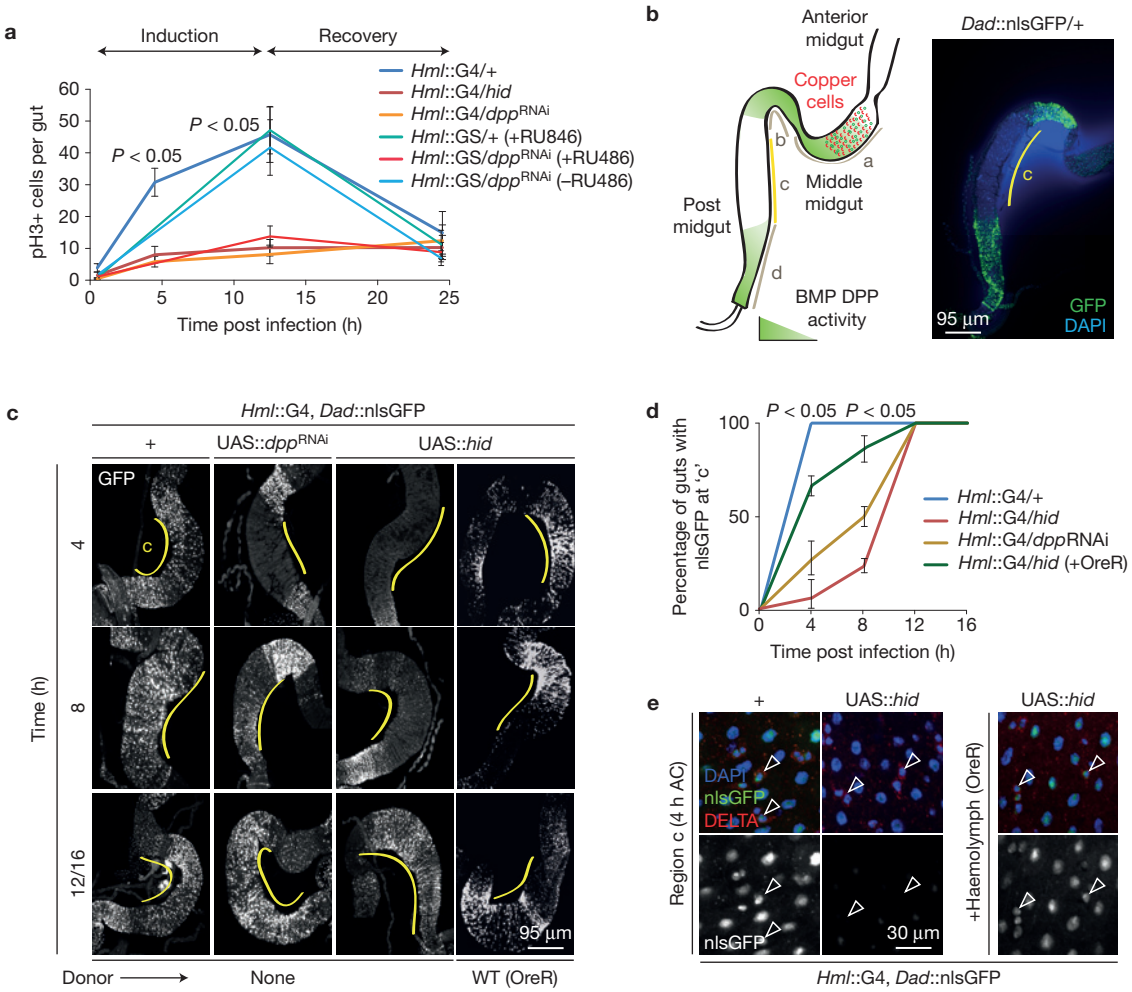

Figure 4 Haemocyte-derived DPP activates BMP signalling specifically within ISCs during proliferation. (**a**) Temporal dynamics of ISC mitotic activity measured as the frequency of phospho-Histone H3+ (pH3+) cells per gut are shown on oral infection with *Ecc*15, with or without *dpp* knockdown in haemocytes using *Hml*Δ::Gal4 or *Hml*Δ::GS drivers. (**b**) Homeostatic expression of *Dad*::nlsGFP in posterior midgut regions of wild-type animals (compare with ref. 18). (**c**–**e**) Expression of *Dad*::nlsGFP is rapidly induced at region c of the midgut in wild-type animals as early as 4 h post-*Ecc*15 challenge (**c**,**d**) in all epithelial cells, including DELTA+ ISCs indicated by arrowheads (**e**), which is delayed in HDD and haemoless flies and is rescued by transplantation of haemolymph from wild-type flies before *Ecc*15 challenge (**c**–**e**). Error bars indicate s.e.m. (**a**: $n=10$; **d**: $n=12$ flies; and data shown are from one experiment that was repeated three times), *P* values from Student's *t*-test. One representative image from 7 flies tested in a single experiment is shown in **b**,**c** and **e**. Experiment was repeated 3 times.

for normal ISC proliferation. Accordingly, loss of *Smox* in ISCs suppressed the growth of ISC tumours formed in Notch loss-of-function conditions[7,8] (Supplementary Fig. 6E). *tkv*, *Medea* (*Med*, the *Drosophila* SMAD4) and *Mad* mutant MARCM clones, on the other hand, either grew bigger or were similar to wild-type controls depending on the alleles tested (Fig. 5d and Supplementary Fig. 6D). On *Ecc*15 infection, however, *tkv* and *Mad* mutant ISCs consistently generated bigger clones than wild-type controls (Fig. 5e, Supplementary Fig. 6D), as observed in previous reports showing that TKV/MAD signalling limits ISC activity following injury[20]. Loss of *sax* or *Smox* suppressed ISC over-proliferation in *tkv* or *Mad* mutant clones (Fig. 5e and Supplementary Fig. 6D), further supporting the notion that SAX/SMOX signalling is an early event required to induce ISC proliferation, and TKV/MAD signalling is a late event, required to ensure recovery to stem cell quiescence once the tissue has been repaired.

We further found that the induction of ISC proliferation by constitutively active EGFR or HOP (hop^{TumL}) is significantly reduced on *Smox* knockdown (Supplementary Fig. 6F). We did not observe enhanced haemocyte recruitment on constitutive expression of active EGFR in ISCs (Supplementary Fig. 6G).

ISC response to DPP is determined by the relative expression of SAX and TKV receptors

The results described above are consistent with recent observations linking SAX to ISC proliferation, and TKV to quiescence[20–22], and suggest a model in which the temporal separation of SAX- and TKV-mediated signalling events dynamically controls ISC proliferation during a regenerative episode. To address how the same DPP ligand could activate two different signalling pathways eliciting opposite proliferative responses within the same stem cells, we assessed the expression of SAX and TKV in ISCs. We reasoned that the relative

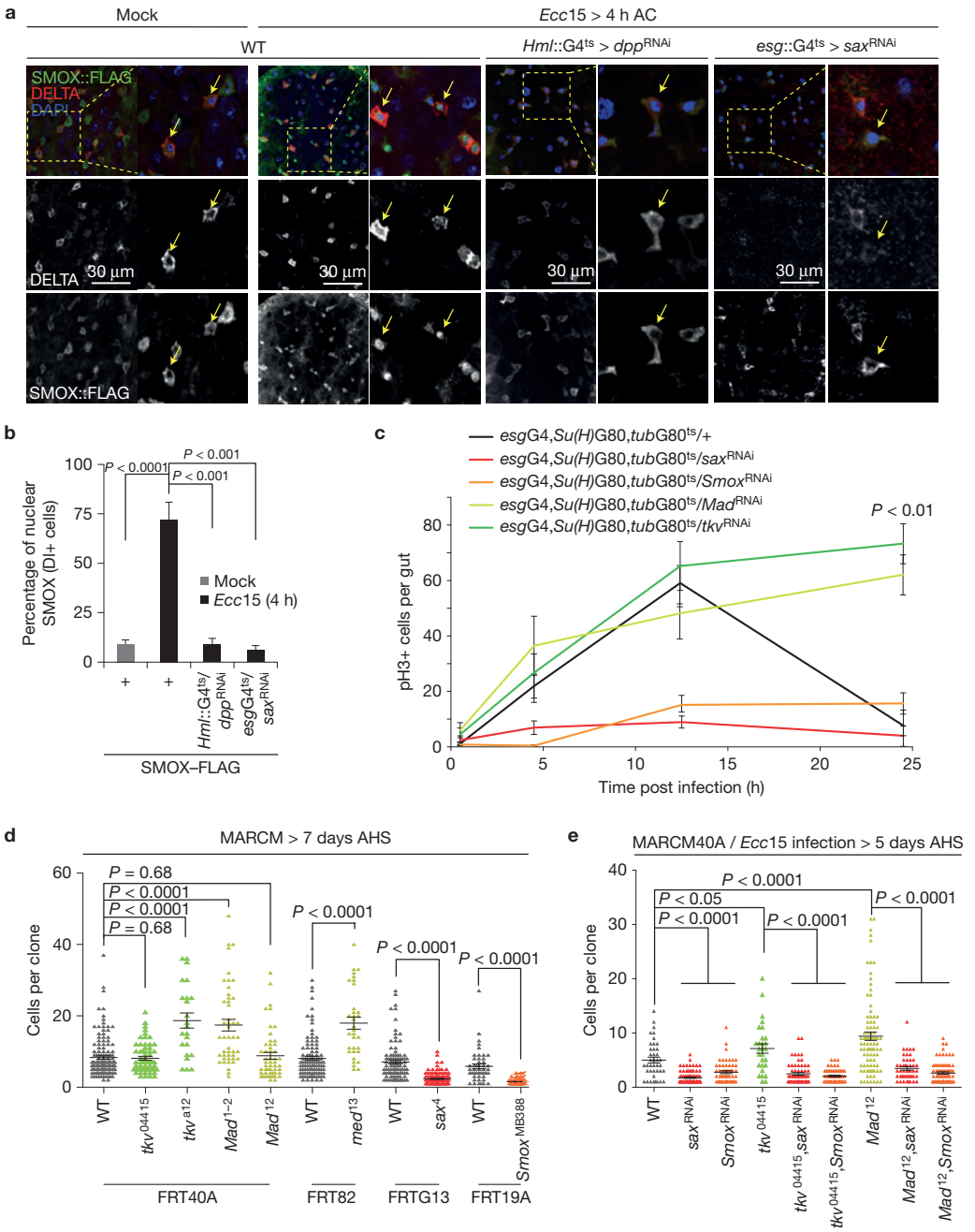

Figure 5 ISC proliferation induced by haemocyte-derived DPP through SAX/SMOX signalling is antagonized by TKV/MAD signalling. (**a**,**b**) SMOX–FLAG is detected in the cytoplasm of DELTA+ cells under homeostatic conditions but is rapidly translocated into the nucleus on *Ecc*15 infection as early as 4 h after challenge (AC). This nuclear translocation of SMOX::FLAG is significantly prevented in HDD flies and in flies where Sax is knocked down specifically in ISCs (**a** and **b**). (**c**) ISC-specific knockdown of *sax* or *Smox* inhibits induction of proliferation and that of *tkv* or *Mad* prevents restoration of quiescence in the fly intestine orally infected by *Ecc*15. (**d**) *sax* or *Smox* mutant clones grow smaller in size (measured as number of cells per clone) but *tkv*, *med* and *Mad* mutant clones either grow bigger or remain comparable to wild-type controls under unstressed conditions. (**e**) *sax* or *Smox* knockdown rescues overgrowth of *tkv* and *Mad* mutant MARCM following *Ecc*15 infection. Error bars indicate s.e.m. (**b**, $n=7$; **c**: $n=15$ flies; and **d**: WT^{FRT40A}, $n=132$; tkv^{04415}, $n=60$; tkv^{a12}, $n=25$; Mad^{1-2}, $n=46$; Mad^{12}, $n=52$, WT^{FRT82}, $n=105$; med^{13}, $n=33$; WT^{FRTG13}, $n=97$; sax^{4}, $n=116$; WT^{FRT19A}, $n=46$; $Smox^{MB388}$, $n=57$; **e**: WT^{FRT40A}, $n=40$; sax^{RNAi}, $n=86$; $Smox^{RNAi}$, $n=55$; tkv^{04415}, $n=28$; tkv^{04415}, sax^{RNAi}, $n=64$; tkv^{04415}, $Smox^{RNAi}$, $n=63$; Mad^{12}, $n=90$; Mad^{12}, sax^{RNAi}, $n=47$; Mad^{12}, $Smox^{RNAi}$, $n=79$ mitotic clones tested from 12 flies, sufficient sample size for MARCM analyses in fly gut[11]; and each experiment is a representative of three (for **b**–**d**) or two (for **e**) independent experiments, *P* values from Student's *t*-test. One representative image from 10 flies is shown in **a**, and experiment was repeated 3 times independently.

expression of these two type I receptors in ISCs in the inductive and recovery phases might influence the response of ISCs to DPP. Indeed, SAX, but not TKV, protein was detected in ISCs under homeostatic conditions (Fig. 6a and Supplementary Fig. 7A,B). During *Ecc*15 infection, on the other hand, SAX expression did not change in ISCs, while TKV expression was low during the inductive phase, but was

induced in ISCs at later stages of the regenerative response (Fig. 6b). SMOX is mostly nuclear during the inductive phase, but translocates to the cytoplasm in the recovery phase, while TKV induction coincides with MAD phosphorylation at the later stage (Fig. 6c and Supplementary Fig. 5C). SAX knockdown in ISCs does not prevent the induction of TKV expression, indicating that DPP/SAX/SMOX signalling is not involved in TKV regulation (Supplementary Fig. 7C).

When wild-type *tkv* was overexpressed in ISCs 6 h before the bacterial challenge, the induction of ISC proliferation was significantly reduced (Fig. 6d), supporting the notion that the induction of TKV expression in the recovery phase switches the ISC response to DPP from inducing proliferation to re-establishing quiescence.

Haemocyte/ISC interactions in infection tolerance and epithelial homeostasis

To examine the physiological consequences of the identified haemocyte/ISC interaction, we assessed host survival in animals orally infected with *PE* (ref. 10), an enteropathogen that induces tissue damage and strongly activates JAK/STAT signalling (Fig. 7b). Flies lacking tissue regeneration rapidly succumbed to PE infection (Fig. 7a), indicating that haemocyte-mediated tissue regeneration contributes to host survival.

In ageing flies, ISCs over-proliferate, causing intestinal dysplasia and contributing to the age-related increase in mortality[9,48,49]. The number of haemocytes attached to the gut in the absence of infection is higher in old than in young flies (Supplementary Fig. 8A), and haemocyte-derived DPP promotes higher *Dad*::nlsGFP expression in region c of the PM in ageing animals (Fig. 7c and Supplementary Fig. 8B). Accordingly, an age-related increase in Smox nuclear localization, which correlates with increased ISC proliferation and dysplasia, is significantly reduced in HDD flies (Fig. 7d,e and Supplementary Figs 1H and 8C,D). These flies have significantly reduced intestinal dysplasia and improved barrier function at 40 days of age (Fig. 7f and Supplementary Fig. 8D), and overexpression of *tkv* in ISCs also reduces the age-related increase in ISC proliferation (Supplementary Fig. 8E). The loss of barrier function has been associated with age-related morbidity and mortality[50], yet we did not observe a change in lifespan of HDD flies as compared to wild-type controls (Supplementary Fig. 8E). Haemoless flies are significantly short-lived, probably owing to the lack of the cellular immune response (Supplementary Fig. 8E).

DISCUSSION

Our results extend the current model for the control of epithelial regeneration in the wake of acute infections in the *Drosophila* intestine (Fig. 8). We propose that the control of ISC proliferation by haemocyte-derived DPP integrates with the previously described regulation of ISC proliferation by local signals from the epithelium and the visceral muscle, allowing precise temporal control of ISC proliferation in response to tissue damage, inflammation and infection.

The association of haemocytes with the intestine is extensive, and can be dynamically increased on infection or damage. In this respect, our observations parallel the invasion of subepithelial layers of the vertebrate intestine by blood cells that induce proliferative responses of crypt stem cells during infection[23]. A role for macrophages and myeloid cells in promoting tissue repair and regeneration has been described in adult salamanders[51] and in mammals[24,25], where TGFβ ligands secreted by these immune cells can inhibit ISC proliferation[52,53], but can also contribute to tumour progression[54]. Our results provide a conceptual framework for immune cell/stem cell interactions in these contexts.

Integration of DPP into the regenerative signalling network in flies

Our observation that DPP/SAX/SMOX signalling is required for UPD-induced proliferation of ISCs suggests that SAX/SMOX signalling cooperates with JAK/STAT and EGFR signalling in the induction of ISC proliferation. Accordingly, while constitutive activation of EGFR/RAS or JAK/STAT signalling in ISCs is sufficient to promote ISC proliferation cell autonomously, we find that this partially depends on Smox. Even in these gain-of-function conditions, ISC proliferation can thus be fully induced only in the presence of basal SMOX activity. As short-term overexpression of DPP in haemocytes does not induce ISC proliferation, we further propose that DPP/SAX/SMOX signalling can activate ISCs only when JAK/STAT and/or EGFR signalling are activated in parallel (Fig. 8). However, long-term overexpression of DPP in haemocytes results in increased ISC proliferation, suggesting that chronic activation of immune cells disrupts normal signalling mechanisms and results in ISC activation even in the absence of tissue damage.

BMP signal transduction in ISCs

BMP TGFβ signalling pathways are critical for metazoan growth and development and have been well characterized in flies. Multiple ligands, receptors and transcription factors with highly context-dependent interactions and function have been described[46,55–59]. This complexity is reflected by the sometimes conflicting studies exploring DPP/TKV/SAX signalling in the adult intestine[18–21]. These studies consistently highlight two important aspects of BMP signalling in the adult *Drosophila* gut: ISCs can undergo opposite proliferative responses to BMP signals; and there are various sources of DPP that differentially influence ISC function in specific conditions. By characterizing the temporal regulation of BMP signalling activity in ISCs, our results resolve some of these conflicts: we propose that early in the regenerative response, haemocyte-derived DPP triggers ISC proliferation by activating SAX/SMOX signalling, and ISC quiescence is re-established by muscle-derived DPP as soon as TKV becomes expressed (Fig. 7). Of note, some of the conflicting conclusions described in the literature may have originated from problems with the genetic tools used in some studies (see Methods). In our study, we have used two independent RNAi lines (BL25782 and BL33618) that effectively decrease *dpp* mRNA levels in haemocytes when expressed using *Hml*Δ::Gal4.

The close association of haemocytes with the type IV collagen Viking suggests that the stimulation of ISC proliferation by haemocyte-derived DPP may also be controlled at the level of ligand availability, as suggested previously for DPP from other sources[21,60].

The regulation of SAX/SMOX signalling by DPP observed here is surprising, but consistent with earlier reports showing that SAX can respond to DPP in certain contexts[46,56]. Biochemical studies have suggested that heterotetrameric complexes between the type II receptor PUNT and the type I receptors SAX and TKV can bind DPP,

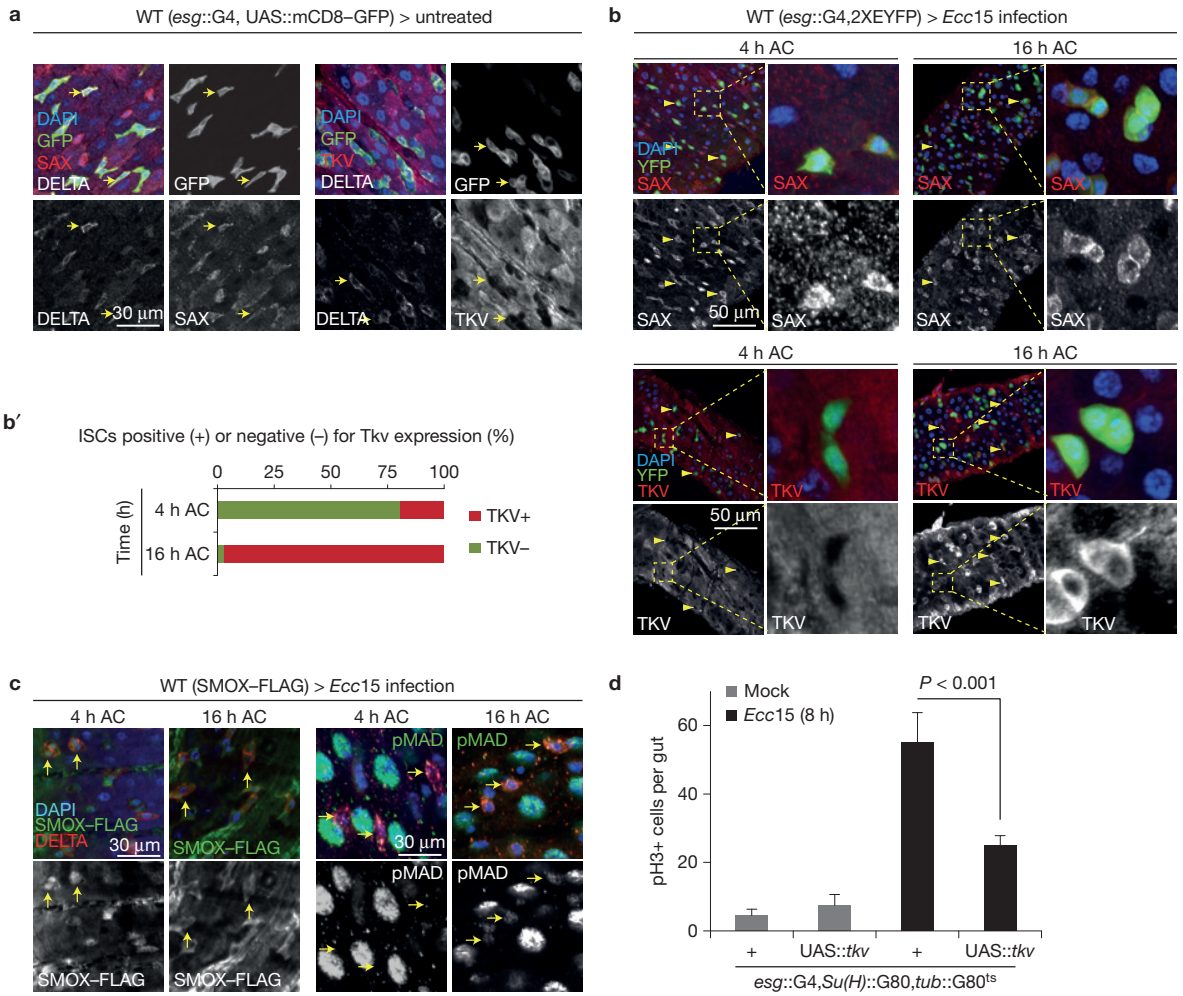

Figure 6 Relative expression of SAX and TKV receptors determines SMOX or MAD activation and proliferative response of ISCs. (**a**,**b**) SAX is highly expressed in ISCs under unstressed conditions (**a**: arrows) as well as all tested stages of *Ecc*15 infection (**b**: arrowheads). TKV expression remains low in ISCs under basal conditions (**a**: arrows) as well as at 4 h of *Ecc*15 challenge (**b**: arrowheads) but high TKV expression is detected in ISCs only at 16 h after *Ecc*15 challenge (AC) (**b**: arrowheads). Panel **b**′ shows the percentage ISCs showing high TKV expression at 4 and 16 h of *Ecc*15 infection. (**c**) Nuclear localization of SMOX detected in ISCs at 4 h is lost on 16 h of infection, and phosphorylation of MAD is detected only at 16 h, but not at 4 h, of *Ecc*15 challenge (arrows). (**d**) Overexpression of wild-type *tkv* in ISCs significantly inhibits the proliferative response induced on *Ecc*15 challenge. Error bars in **d** indicate s.e.m. (data from $n=7$ flies tested in one experiment, P values from Student's t-test); and experiment was performed 3 times independently. One representative images from 7 flies used in each experiment is shown in **a**–**c**; and every experiment was reproduced three times independently.

and complexes with TKV/TKV homodimers preferentially bind DPP, and complexes with SAX/SAX homodimers preferentially bind GBB (ref. 58). In the absence of TKV, SAX has been proposed to sequester GBB, shaping the GBB activity gradient, but to fail to signal effectively[46]. Expression of GBB in the midgut epithelium has recently been described, and ligand heterodimers between GBB and DPP are well established[21,57]. Consistent with earlier reports[21,22], we find that GBB knockdown in ECs significantly reduces ISC proliferation in response to infection. Complex interactions between haemocyte-derived DPP, epithelial GBB, and ISC-expressed SAX, PUNT and TKV thus probably shape the response of ISCs to damage, and will be an interesting area of further study.

Similar complexities exist in the regulation of transcription factors by SAX and TKV. Canonically, SMOX is regulated by Activin ligands (Activin, Dawdle, Myoglianin and maybe more), and the type I receptor Baboon[55]. We have tested the role of Activin and Dawdle in ISC regulation, and, in contrast to DPP, were unable to detect a requirement for these factors in the induction of ISC proliferation after *Ecc*15 infection. Furthermore, our data establish a requirement for haemocyte-derived DPP as well as for SAX expression in ISCs in the nuclear translocation of SMOX after a challenge. Our study thus indicates that in this context, SAX responds to DPP and regulates SMOX. Regulation of SMOX by SAX has been described before[61], yet SAX is also known to promote MAD phosphorylation, but only in the presence of TKV (ref. 46). Consistent with such observations, we have detected MAD phosphorylation in ISCs only in the late recovery phase on bacterial infection, when TKV is simultaneously induced in ISCs. During this recovery phase, ISCs maintain high SAX expression, but SMOX nuclear localization is not detected anymore, suggesting that SAX cannot activate SMOX in the presence of TKV, and might actually divert signals towards MAD instead, as previously suggested[46]. Our data also suggest that Medea (the *Drosophila* SMAD4 homologue) is

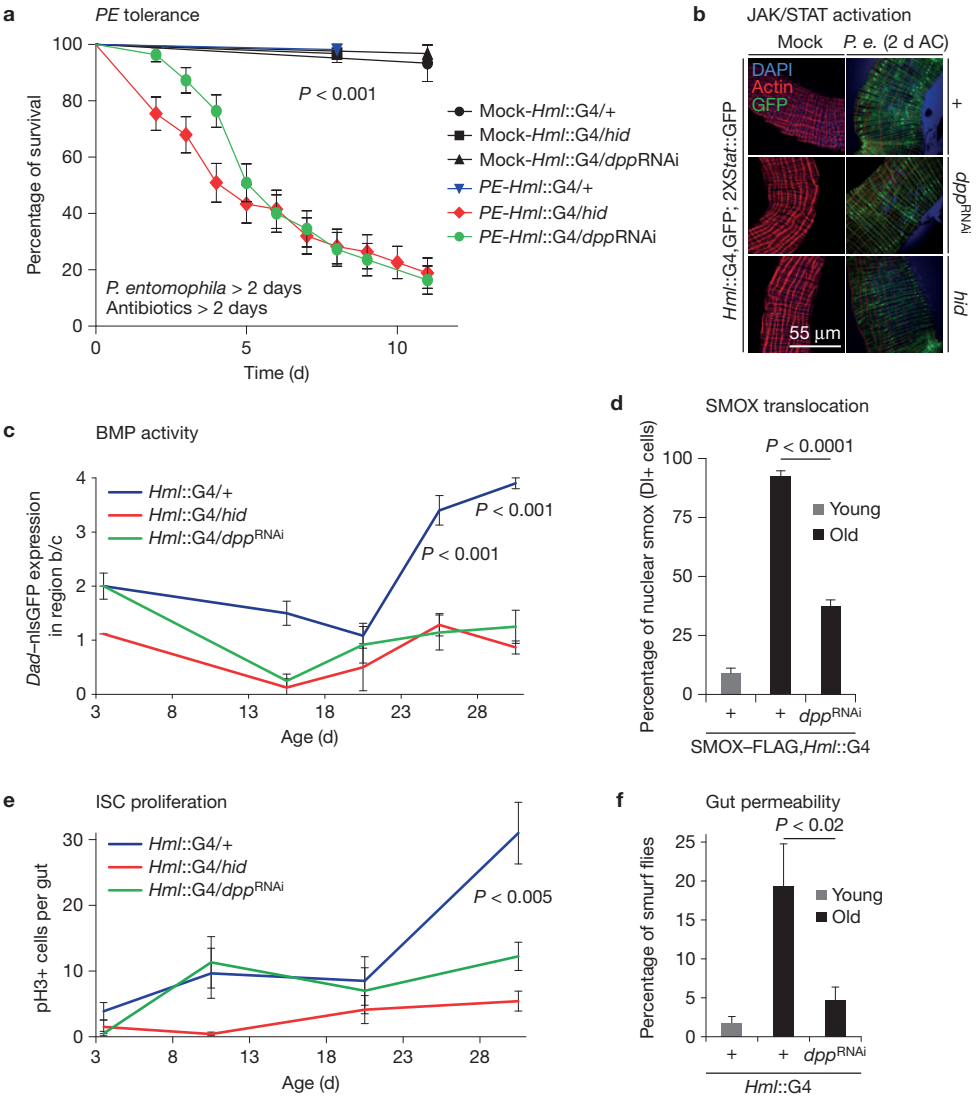

Figure 7 Haemocyte-derived DPP promotes resistance to acute infection but leads to intestinal dysplasia and increased gut permeability during ageing. (**a**) Haemoless and HDD flies rapidly succumb to acute intestinal damage. Survival rates of flies were monitored after a prior feeding on *PE* or Mock for 2 days followed by 2 days of antibiotics treatment. (**b**) Induction of STAT::GFP reporter expression in the gut of haemoless and HDD flies 2 days post-*PE* infection is similar to wild-type controls. (**c**) Expression of *Dad*::nlsGFP both at regions b and c of the PM is shown in ageing flies (individual guts were given a score (0–4) for the strength of *Dad*:nGFP gradient at regions b and c of PM: 0 = no GFP signal; 1 = short gradient at region b; 2 = normal gradient at region b; 3 = long gradient at region b that penetrates into region c; 4 = high and evenly expressed GFP signal throughout both regions b and c). (**d**,**e**) Age-related induction of *Dad*::nlsGFP expression correlates with enhanced nuclear translocation of Smox in DELTA-positive ISCs located in region c (**d**) as well as with the increased ISC proliferation (**e**). All of these phenotypes are dependent on haemocyte-derived DPP (**c**–**e**). (**f**) HDD flies exhibit improved intestinal epithelial integrity. *P* values from log rank test in **a** (calculated using Prism software). Other *P* values from Student's *t*-test. Error bars indicate s.e.m. (**a**: $n=40$; **c**: $n=8$; **d**: $n=7$; **e**: $n=18$; **f**: $n=150$ flies tested in one experiment; and each experiment was reproduced 3 (in **e**) or 2 times (in **c**,**d** and **f**)). One representative image from 10 flies is shown in **b**; and experiment was repeated twice.

not required for SMOX activity. Although surprising, this observation is consistent with recent reports that SMAD proteins in mammals can translocate into the nucleus and activate target genes in a SMAD4-independent manner[62]. The specific signalling readouts in ISCs when these cells are exposed to various BMP ligands and are expressing different combinations of receptors are thus likely to be complex.

Haemocyte/ISC interactions, infection tolerance, and ageing

Our findings demonstrate that the control of ISC proliferation by haemocyte-derived DPP is critical for tolerance against enteropathogens, but contributes to ageing-associated epithelial dysfunction, highlighting the importance of tightly controlled interactions between blood cells and stem cells in this tissue. Nevertheless, where haemocytes themselves are required for normal lifespan, loss of haemocyte-derived DPP does not impact lifespan. One interpretation of this finding is that beneficial (improved gut homeostasis) and deleterious (for example, reduced immune competence of the gut epithelium) consequences of reduced haemocyte-derived DPP cancel each other out over the lifespan of the animal. It will be interesting to test this hypothesis in future studies.

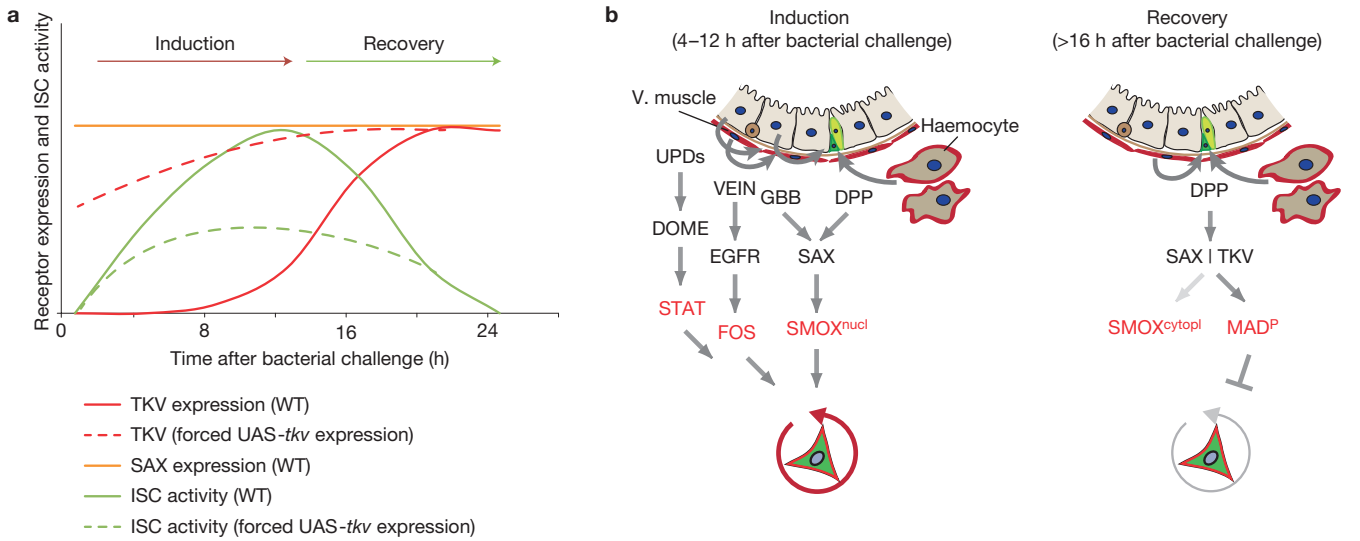

Figure 8 Model. (**a**) Proposed relationship between SAX/TKV expression and ISC proliferation during one regeneration episode. (**b**) Model for the dynamic control of ISC activity by haemocyte- and muscle-derived DPP during the regenerative response. Under basal conditions, SAX, but not TKV, is expressed in ISCs. In response to infection or damage, haemocyte-derived DPP and EC-derived GBB signal through SAX to activate SMOX, which requires active STAT and FOS to induce ISC proliferation ('inductive phase'). Subsequent induction of TKV expression in ISCs is required for the 'recovery phase', where haemocyte- and muscle-derived DPP and EC-derived GBB signal through TKV and SAX to induce MAD signalling to restore stem cell quiescence.

Ageing is associated with systemic inflammation, and a role for immune cells in promoting inflammation in ageing vertebrates has been proposed[63,64]. In humans, recruitment of immune cells to the gut is required for proper stem cell proliferation in response to luminal microbes[23], and prolonged inflammatory bowel disease further contributes to cancer development[65]. It is thus anticipated that conserved macrophage/stem cell interactions influence the aetiology and progression of such diseases. Our data confirm a role for haemocytes in age-related intestinal dysplasia in the fly intestine, and provide mechanistic insight into the causes for this deregulation. It can be anticipated that similar interactions between macrophages and intestinal stem cells may contribute to the development of IBDs, intestinal cancers, and general loss of homeostasis in the ageing human intestine. □

METHODS

Methods and any associated references are available in the online version of the paper.

Note: Supplementary Information is available in the online version of the paper

ACKNOWLEDGEMENTS

This work was financially supported by the National Institute on General Medical Sciences (R01 GM100196) and the National Eye Institute (R01 EY018177). We would like to thank J. Karpac for comments.

AUTHOR CONTRIBUTIONS

A.A. and H.J. designed all experiments. A.A. generated transgenic animals and performed experiments on haemocytes, DPP, SAX and SMOX signalling, interactions of SAX/SMOX signalling with TKV/MAD, EGFR and JAK/STAT pathways and role of TKV expression in mitosis and on ageing, dysplasia and lifespan; H.L. validated specificity of TKV and SAX antibodies, performed experiments on TKV expression and on lineage tracing of MAD, MED and TKV mutant ISCs, and provided additional reagents for other experiments. A.A. and H.J. analysed the data and wrote the manuscript.

COMPETING FINANCIAL INTERESTS

The authors declare no competing financial interests.

Published online at http://dx.doi.org/10.1038/ncb3174
Reprints and permissions information is available online at www.nature.com/reprints

1. Ferrandon, D. The complementary facets of epithelial host defenses in the genetic model organism *Drosophila melanogaster*: from resistance to resilience. *Curr. Opin. Immunol.* **25,** 59–70 (2013).
2. Lemaitre, B. & Miguel-Aliaga, I. The digestive tract of *Drosophila melanogaster*. *Annu. Rev. Genet.* **47,** 377–404 (2013).
3. Ostaff, M. J., Stange, E. F. & Wehkamp, J. Antimicrobial peptides and gut microbiota in homeostasis and pathology. *EMBO Mol. Med.* **5,** 1465–1483 (2013).
4. Kaiko, G. E. & Stappenbeck, T. S. Host–microbe interactions shaping the gastrointestinal environment. *Trends Immunol.* **35,** 538–548 (2014).
5. Buchon, N., Broderick, N. A. & Lemaitre, B. Gut homeostasis in a microbial world: insights from *Drosophila melanogaster*. *Nat. Rev. Microbiol.* **11,** 615–626 (2013).
6. Ayyaz, A. & Jasper, H. Intestinal inflammation and stem cell homeostasis in aging. *Front. Cell. Infect. Microbiol.* **3,** 98 (2013).
7. Micchelli, C. A. & Perrimon, N. Evidence that stem cells reside in the adult *Drosophila* midgut epithelium. *Nature* **439,** 475–479 (2006).
8. Ohlstein, B. & Spradling, A. The adult *Drosophila* posterior midgut is maintained by pluripotent stem cells. *Nature* **439,** 470–474 (2006).
9. Biteau, B., Hochmuth, C. E. & Jasper, H. Maintaining tissue homeostasis: dynamic control of somatic stem cell activity. *Cell Stem Cell* **9,** 402–411 (2011).
10. Jiang, H. *et al.* Cytokine/Jak/Stat signaling mediates regeneration and homeostasis in the *Drosophila* midgut. *Cell* **137,** 1343–1355 (2009).
11. Biteau, B. & Jasper, H. EGF signaling regulates the proliferation of intestinal stem cells in *Drosophila*. *Development* **138,** 1045–1055 (2011).
12. Xu, N. *et al.* EGFR, Wingless and JAK/STAT signaling cooperatively maintain *Drosophila* intestinal stem cells. *Dev. Biol.* **354,** 31–43 (2011).
13. Buchon, N., Broderick, N. A., Kuraishi, T. & Lemaitre, B. *Drosophila* EGFR pathway coordinates stem cell proliferation and gut remodeling following infection. *BMC Biol.* **8,** 152 (2010).
14. Jiang, H., Grenley, M. O., Bravo, M. J., Blumhagen, R. Z. & Edgar, B. A. EGFR/Ras/MAPK signaling mediates adult midgut epithelial homeostasis and regeneration in *Drosophila*. *Cell Stem Cell* **8,** 84–95 (2011).
15. Buchon, N., Broderick, N. A., Chakrabarti, S. & Lemaitre, B. Invasive and indigenous microbiota impact intestinal stem cell activity through multiple pathways in *Drosophila*. *Genes Dev.* **23,** 2333–2344 (2009).
16. Cronin, S. J. F. *et al.* Genome-wide RNAi screen identifies genes involved in intestinal pathogenic bacterial infection. *Science* **325,** 340–343 (2009).
17. Cordero, J. B. & Sansom, O. J. Wnt signalling and its role in stem cell-driven intestinal regeneration and hyperplasia. *Acta Physiol.* **204,** 137–143 (2012).
18. Li, H., Qi, Y. & Jasper, H. Dpp signaling determines regional stem cell identity in the regenerating adult *Drosophila* gastrointestinal tract. *Cell Rep.* **4,** 10–18 (2013).

19. Li, Z., Zhang, Y., Han, L., Shi, L. & Lin, X. Trachea-derived dpp controls adult midgut homeostasis in *Drosophila*. *Dev. Cell* **24,** 133–143 (2013).
20. Guo, Z., Driver, I. & Ohlstein, B. Injury-induced BMP signaling negatively regulates *Drosophila* midgut homeostasis. *J. Cell Biol.* **201,** 945–961 (2013).
21. Tian, A. & Jiang, J. Intestinal epithelium-derived BMP controls stem cell self-renewal in *Drosophila* adult midgut. *eLife* **3,** e01857 (2014).
22. Zhou, J. *et al.* Dpp/Gbb signaling is required for normal intestinal regeneration during infection. *Dev. Biol.* **399,** 189–203 (2014).
23. Skoczek, D. A. *et al.* Luminal microbes promote monocyte–stem cell interactions across a healthy colonic epithelium. *J. Immunol.* **193,** 439–451 (2014).
24. Pull, S. L., Doherty, J. M., Mills, J. C., Gordon, J. I. & Stappenbeck, T. S. Activated macrophages are an adaptive element of the colonic epithelial progenitor niche necessary for regenerative responses to injury. *Proc. Natl Acad. Sci. USA* **102,** 99–104 (2005).
25. Malvin, N. P., Seno, H. & Stappenbeck, T. S. Colonic epithelial response to injury requires Myd88 signaling in myeloid cells. *Mucosal Immunol.* **5,** 194–206 (2012).
26. Lemaitre, B. & Hoffmann, J. The host defense of *Drosophila melanogaster*. *Annu. Rev. Immunol.* **25,** 697–743 (2007).
27. Babcock, D. T. *et al.* Circulating blood cells function as a surveillance system for damaged tissue in *Drosophila* larvae. *Proc. Natl Acad. Sci. USA* **105,** 10017–10022 (2008).
28. Charroux, B. & Royet, J. Elimination of plasmatocytes by targeted apoptosis reveals their role in multiple aspects of the *Drosophila* immune response. *Proc. Natl Acad. Sci. USA* **106,** 9797–9802 (2009).
29. Zaidman-Remy, A., Regan, J. C., Brandao, A. S. & Jacinto, A. The *Drosophila* larva as a tool to study gut-associated macrophages: PI3K regulates a discrete hemocyte population at the proventriculus. *Dev. Comp. Immunol.* **36,** 638–647 (2012).
30. Tokusumi, T., Shoue, D. A., Tokusumi, Y., Stoller, J. R. & Schulz, R. A. New hemocyte-specific enhancer-reporter transgenes for the analysis of hematopoiesis in *Drosophila*. *Genesis* **47,** 771–774 (2009).
31. Kurucz, E. *et al.* Nimrod, a putative phagocytosis receptor with EGF repeats in *Drosophila* plasmatocytes. *Curr. Biol.* **17,** 649–654 (2007).
32. Amcheslavsky, A., Jiang, J. & Ip, Y. T. Tissue damage-induced intestinal stem cell division in *Drosophila*. *Cell Stem Cell* **4,** 49–61 (2009).
33. Makhijani, K., Alexander, B., Tanaka, T., Rulifson, E. & Bruckner, K. The peripheral nervous system supports blood cell homing and survival in the *Drosophila* larva. *Development* **138,** 5379–5391 (2011).
34. Lee, T. & Luo, L. Mosaic analysis with a repressible cell marker (MARCM) for *Drosophila* neural development. *Trends Neurosci.* **24,** 251–254 (2001).
35. Zettervall, C. J. *et al.* A directed screen for genes involved in *Drosophila* blood cell activation. *Proc. Natl Acad. Sci. USA* **101,** 14192–14197 (2004).
36. Clark, R. I., Woodcock, K. J., Geissmann, F., Trouillet, C. & Dionne, M. S. Multiple TGF-β superfamily signals modulate the adult *Drosophila* immune response. *Curr. Biol.* **21,** 1672–1677 (2011).
37. Teleman, A. A. & Cohen, S. M. Dpp gradient formation in the *Drosophila* wing imaginal disc. *Cell* **103,** 971–980 (2000).
38. Harrison, D. A. & Perrimon, N. Simple and efficient generation of marked clones in *Drosophila*. *Curr. Biol.* **3,** 424–433 (1993).
39. Bardet, P. L. *et al.* A fluorescent reporter of caspase activity for live imaging. *Proc. Natl Acad. Sci. USA* **105,** 13901–13905 (2008).
40. Hamaratoglu, F., de Lachapelle, A. M., Pyrowolakis, G., Bergmann, S. & Affolter, M. Dpp signaling activity requires Pentagone to scale with tissue size in the growing *Drosophila* wing imaginal disc. *PLoS Biol.* **9,** e1001182 (2011).
41. Brummel, T. J. *et al.* Characterization and relationship of Dpp receptors encoded by the saxophone and thick veins genes in *Drosophila*. *Cell* **78,** 251–261 (1994).
42. Henderson, K. D. & Andrew, D. J. Identification of a novel *Drosophila* SMAD on the X chromosome. *Biochem. Biophys. Res. Commun.* **252,** 195–201 (1998).
43. Spokony, R. & White, K. *Spokony Insertions* (Flybase, 2013).
44. Zhu, C. C. *et al.* *Drosophila* Activin- and the Activin-like product Dawdle function redundantly to regulate proliferation in the larval brain. *Development* **135,** 513–521 (2008).
45. Kim, M. J. & O'Connor, M. B. Anterograde activin signaling regulates postsynaptic membrane potential and GluRIIA/B abundance at the *Drosophila* neuromuscular junction. *PLoS ONE* **9,** e107443 (2014).
46. Bangi, E. & Wharton, K. Dual function of the *Drosophila* Alk1/Alk2 ortholog Saxophone shapes the Bmp activity gradient in the wing imaginal disc. *Development* **133,** 3295–3303 (2006).
47. Haerry, T. E., Khalsa, O., O'Connor, M. B. & Wharton, K. A. Synergistic signaling by two BMP ligands through the SAX and TKV receptors controls wing growth and patterning in *Drosophila*. *Development* **125,** 3977–3987 (1998).
48. Biteau, B. *et al.* Lifespan extension by preserving proliferative homeostasis in *Drosophila*. *PLoS Genet.* **6,** e1001159 (2010).
49. Guo, L., Karpac, J., Tran, S. L. & Jasper, H. PGRP-SC2 promotes gut immune homeostasis to limit commensal dysbiosis and extend lifespan. *Cell* **156,** 109–122 (2014).
50. Rera, M., Clark, R. I. & Walker, D. W. Intestinal barrier dysfunction links metabolic and inflammatory markers of aging to death in *Drosophila*. *Proc. Natl Acad. Sci. USA* **109,** 21528–21533 (2012).
51. Godwin, J. W., Pinto, A. R. & Rosenthal, N. A. Macrophages are required for adult salamander limb regeneration. *Proc. Natl Acad. Sci. USA* **110,** 9415–9420 (2013).
52. Assoian, R. K. *et al.* Expression and secretion of type β transforming growth factor by activated human macrophages. *Proc. Natl Acad. Sci. USA* **84,** 6020–6024 (1987).
53. Miyoshi, H., Ajima, R., Luo, C. T., Yamaguchi, T. P. & Stappenbeck, T. S. Wnt5a potentiates TGF-β signaling to promote colonic crypt regeneration after tissue injury. *Science* **338,** 108–113 (2012).
54. Wakefield, L. M. & Hill, C. S. Beyond TGFβ: roles of other TGFβ superfamily members in cancer. *Nat. Rev. Cancer* **13,** 328–341 (2013).
55. Peterson, A. J. & O'Connor, M. B. Strategies for exploring TGF-β signaling in *Drosophila*. *Methods* **68,** 183–193 (2014).
56. Twombly, V. *et al.* Functional analysis of saxophone, the *Drosophila* gene encoding the BMP type I receptor ortholog of human ALK1/ACVRL1 and ACVR1/ALK2. *Genetics* **183,** 563–579 (2009) 1SI-8SI.
57. Bangi, E. & Wharton, K. Dpp and Gbb exhibit different effective ranges in the establishment of the BMP activity gradient critical for *Drosophila* wing patterning. *Dev. Biol.* **295,** 178–193 (2006).
58. Haerry, T. E. The interaction between two TGF-β type I receptors plays important roles in ligand binding, SMAD activation, and gradient formation. *Mech. Dev.* **127,** 358–370 (2010).
59. Brummel, T. *et al.* The *Drosophila* activin receptor baboon signals through dSmad2 and controls cell proliferation but not patterning during larval development. *Genes Dev.* **13,** 98–111 (1999).
60. Wang, X., Harris, R. E., Bayston, L. J. & Ashe, H. L. Type IV collagens regulate BMP signalling in *Drosophila*. *Nature* **455,** 72–77 (2008).
61. Li, C. Y., Guo, Z. & Wang, Z. TGFβ receptor saxophone non-autonomously regulates germline proliferation in a Smox/dSmad2-dependent manner in *Drosophila* testis. *Dev. Biol.* **309,** 70–77 (2007).
62. Isogaya, K. *et al.* A Smad3 and TTF-1/NKX2-1 complex regulates Smad4-independent gene expression. *Cell Res.* **24,** 994–1008 (2014).
63. Shaw, A. C., Goldstein, D. R. & Montgomery, R. R. Age-dependent dysregulation of innate immunity. *Nat. Rev. Immunol.* **13,** 875–887 (2013).
64. Wang, G. C. & Casolaro, V. Immunologic changes in frail older adults. *Transl. Med. UniSa* **9,** 1–6 (2014).
65. Khor, B., Gardet, A. & Xavier, R. J. Genetics and pathogenesis of inflammatory bowel disease. *Nature* **474,** 307–317 (2011).

METHODS

Fly lines and husbandry. Flies were cultured on yeast/molasses-based food at 25 °C with a 12 h light/dark cycle and only female animals were used in all experiments.

The following fly lines were used: W^{1118} (WT), y^1w^1, FRT40, FRTG13, FRT82, upd1^{RNAi} (BL28722), upd2^{RNAi} (BL33949), upd3^{RNAi} (BL28575), Dpp$^{RNAi\ \#1}$ (BL33618; ref. 18), Dpp$^{RNAi\ \#2}$ (BL25782), Sax^{RNAi} (BL36131; ref. 21), Smox^{RNAi} (BL26756), Mad^{RNAi} (BL31315), Gbb^{RNAi} (BL34898; refs 21,22), UAS::Dpp (BL1486), UAS::Tkv (BL51653), UAS::Tkv^{QD} (BL36536; ref. 18), UAS::CD8-GFP (BL5137), UAS::rpr (BL5823), Smox::FLAG (BL43958), EGFR-GOF (BL9536: p{Egfr.1.A887T.UAS}c12-7), Mad1-2,FRT40/cyo (BL7323), Med13,FRT82/TM3 (BL7340), Sax4,FRTG13/cyo (BL5404), SmoxMB388,FRT19A/FM7c (BL44384), tubG80^{ts} (BL7017 and BL7108), hmlΔ::Gal4,UAS::GFP (BL30140, BL30142), hmlΔ::Gal4 (BL30141), p[He-Gal4] (BL8699), Dpp:Gal4 (BL1553), Dpp::Gal4^{Gut} (BL45111; ref. 20), How::Gal4 (BL1767), all provided by Bloomington Drosophila Stock Center. Tkv^{RNAi} (vdrc3059), Spi^{RNAi} (vdrc103817), Vein^{RNAi} (vdrc109437), STAT^{RNAi} (vdrc106980), pvf1^{RNAi} (vdrc46875), pvf2^{RNAi} (vdrc7629), Bsk^{RNAi} (vdrc34138), and Keren^{RNAi} (vdrc104299) were obtained from the Vienna Drosophila RNAi Center. Cardia–Gal4 (103522), dve::Gal4 (113273) and UAS::Sax (F001576) were obtained from Drosophila Genomics Resource Center (DGRC) and FlyORF (Zurich ORFeome Project), respectively. The line UAS::hid was a gift from J. K. Billeter (University of Groningen, Netherlands), dad::nlsGFP from G. Pyrowolakis (University of Freiburg, Germany), UAS::DppGFP from A. Lander (UC, Irvine, USA), Vkg–GFP from B. Biteau[11] (University of Rochester, USA), Mad12,FRT40/cyo, Tkv8,FRT40/cyo (ref. 18), 5966::GeneSwitch[49], MARCM40A and MARCM82A from B. Ohlstein (Columbia University, USA), tkva12,FRT40/cyo (ref. 18), Btl::Gal4^{ts} from D. Bohmann (University of Rochester, USA), byn-Gal4 from V. Hartenstien (UCLA, USA), Eater::DsRed from T. Tokusumi[30] (University of Notre Dame, USA), NP1G80^{ts} from D. Ferrandon[16] (IBMC, France), esg::Gal4 (ref. 49), UAS::GFP from S. Hayashi (RIKEN, Japan), esg::Gal4,Su(H)GBE::G80,UAS::2XEYFP,tub::G80^{ts} from S. Hou[66] (NIH, USA), hmlΔ::RFP from K. Bruckner[33] (UCSF, USA), tkv8,FRT40/cyo, tkv04415,FRT40/cyo (ref. 20), Notch^{RNAi}, hsFlp, yw; X.15.29 and yw; X.15.33 (ref. 38) from N. Perrimon (Harvard, USA), 2XSTAT::GFP from E.A. Bach (New York University, USA), UAS::HopTumL from D. Bilder (UC, Berkeley, USA), and UAS::upd2 from M. Zeidler (The University of Sheffield, UK). hmlΔ::GeneSwitch and hmlΔ::Dpp^{RNAi} were made in this study. Haemoless and HDD flies were made by crossing the hml::Gal4,UAS::GFP line with UAS::hid and Dpp^{RNAi}, respectively, and animals were allowed to develop at 25 °C. Also see Supplementary Table 1 for specific genotypes used for individual experiments in each figure.

Generation of transgenic animals. To construct the hmlΔ::GeneSwitch line, a ~839 bp fragment was amplified from crude DNA of *w1118* flies using primer sequences: Fw, 5′-ACGCGTCAAAAGTTATTTCTGTAGGC-3′; Rev, 5-′ACGCG TTTTGTTAGGCTAATCGGAAATTG-3′ (also see ref. 33). The resulting hmlΔ promoter fragment was cloned into the pP[UAS-GeneSwitch] vector[67] at a single MluI restriction site. To generate hmlΔ::Dpp^{RNAi} transgenic animals, a ~1.5 kbp DNA fragment containing the Dpp hairpin was amplified from DNA extract of a UAS::Dpp^{RNAi} fly line generated at Transgenic RNAi Project (TRiP): TRiP no. HMS00011 (Hairpin ID: SH.00007.N); Bloomington Stock no. 33618 (also see ref. 68 for construction of the original TRiP fly line and the specificity of the hairpin construct against Dpp), using primer sequences: Fw, agg cct tct agc agt 5′-TCGT TCAGTGATAGTGATAAA-3′ tag tta tat tca agc ata; and Rev, aac cgg ttg ttg ttg gtt ggc aca cca caa ata tac tg; where the actual Dpp short hairpin sequence is shown in capital letters. The resulting Dpp^{RNAi} fragment was then cloned into the StuI/AgeI sites of the *hml Δ::pRed H-Pelican* vector, a gift from K. Brueckner[33] (UCSF, USA), to generate the *hml Δ::Dpp^{RNAi}-pRed H-Pelican* vector. Transgenic flies were generated by standard procedures (Genetic Services).

Selection of Dpp^{RNAi} lines. A recent study[21] has reported contradictory effects of Dpp on ISC proliferation and self-renewal when Dpp was knocked down in ECs using two different RNAi lines: Bloomington Stock Number 33628, termed DppRNAi^S by the authors, and Bloomington Stock Number 25782 (called DppRNAi^W). A recent comment on flybase.com explains, however, that, based on flybase release 5.43, DppRNAi^S (Bloomington Number 33628) does not match Dpp transcripts accurately (http://flystocks.bio.indiana.edu/Reports/33628.html), but the DppRNAi^W line (Bloomington Number BL25782) and a third DppRNAi line (Bloomington Number BL33618) specifically target Dpp transcripts and have no reported off targets. Both of the later lines efficiently knock down Dpp transcripts (Supplementary Fig. 3E) yet do not inhibit ISC proliferation during stress when expressed by an EC-specific driver[21] (Supplementary Fig. 3D). Owing to their target specificity, we have used these two lines in our analyses.

Immunostaining and microscopy. Adult female *Drosophila* guts were dissected in 1× phosphate-buffered saline (PBS), fixed for 45 min at room temperature in fixative (100 mM glutamic acid, 25 mM KCl, 20 mM $MgSO_4$, 4 mM sodium phosphate, 1 mM $MgCl_2$, and 4% formaldehyde), washed for 1 h at 4 °C in washing buffer (×1 PBS, 0.5% bovine serum albumin and 0.1% Triton X-100), and then incubated in primary antibodies (4 °C overnight) and secondary antibodies (4 °C for 4 h or overnight) in washing buffer, between which was 1 h washing at 4 °C. Staining with pSMad3 antibody was performed using a phosphatase inhibitor (Roche, 4906837001) during fixation, 1 h wash, and primary antibody incubation following the same protocol above. Staining with Delta and FLAG antibodies was performed following the methanol–heptane fixation method described in ref. 18.

To monitor dynamics of haemocyte attachment to the intestine, flies were held with thin entomological pins in Sylgard-coated small Petri dish and dissected directly into fixation solution (100 mM glutamic acid, 25 mM KCl, 20 mM $MgSO_4$, 4 mM sodium phosphate, 1 mM $MgCl_2$ and 4% formaldehyde). Forceps were used to gently remove dorsal cuticle to expose the body cavity to fixative for at least one hour. Observations were then made either directly under fluorescent microscope or opened animals were incubated in a described staining solution. Animals were finally washed 3× and guts were carefully removed, preserving all tissues attached to the gut, and mounted to perform confocal microscopy. To examine the morphology of circulating haemocytes (Supplementary Fig. 2D), haemolymph was collected in PBS (as described below) from 20 flies and transferred to glass slides. Haemocytes were then allowed to settle for 30 min at room temperature followed by fixation for 15 min and subsequent incubation in phalloidin solution overnight at 4 °C.

Primary antibodies and dilution: rabbit anti-pSMad3 (Epitomics, 1:300), rabbit anti-β-galactosidase (Cappel, 1:5,000), rabbit anti-GFP (Invitrogen, 1:500), rabbit anti-phospho-Histone H3 Ser 10 (Upstate, 1:1,000), mouse anti-Prospero (Developmental Studies Hybridoma Bank, DSHB, 1:250), mouse monoclonal anti-Cut (DSHB, 1:100), mouse anti-Armadillo (DSHB, 1:100), rabbit anti-Sax (abcam, ab42105, 1:200), rabbit anti-FLAG (Sigma, 1:300), rat anti-Delta (gift from M. Rand, University of Vermont, USA, 1:1,000), mouse anti-NimC1 (gift from I. Andó, Hungarian Academy of Sciences, Hungary, 1:30; ref. 31) and rabbit anti-Tkv (gift from M. Gonzalez-Gaitan, University of Geneva, Switzerland, 1:100). Fluorescent secondary antibodies were from Jackson Immunoresearch. DAPI was used to stain DNA and phalloidin (Invitrogen) to stain actin. The images of whole flies were taken on a Zeiss dissecting fluorescent microscope, and all other images were taken on a Zeiss LSM 700 confocal microscope and processed using Adobe Photoshop, Illustrator and Image J.

Conditional expression of UAS-linked transgenes. The TARGET system was used in combination with the indicated Gal4 driver to conditionally express UAS-linked transgenes[69]. Flies were developed at 18 °C, and then shifted to 29 °C to induce transgene expression. For GeneSwitch drivers, flies were developed on normal food at 25 °C and 2–5-day-old adults were transferred to mifepristone (RU486)-containing food for 2 days before performing experiments.

Bacterial infection, Paraquat treatment and feeding assays. Previously described procedures[10,13,15] were followed for oral bacterial challenge. Briefly, the bacterial strains, *Ecc*15 or *Pseudomonas entomophila* (*PE*), were cultured in LB medium overnight at 30 °C. Flies were fed on 500 µl of concentrated bacteria in 5% sucrose (OD100) for the time indicated and the same volume of 5% sucrose as a control. To test feeding efficiency, 5% bromophenol blue was mixed in infection solution before flies were transferred to feed for 90 min. CAFÉ assay was performed as described previously[18]. For Paraquat exposure, flies were fed on either 5 mM Paraquat in 5% sucrose solution or only on 5% sucrose as a control, for an indicated time. In the case of each of the above treatments, flies were starved in empty vials for 2 h. For survival experiments, flies were either orally infected with *PE* for 2 days and shifted for another 2 days to a cocktail of antibiotics as described previously[10], before starting to monitor the rate of fly survival (Fig. 7a), or a tungsten needle was used to directly inject *PE* into fly haemolymph as described in ref. 28, followed by monitoring their survival (Supplementary Fig. 1F).

Haemolymph extraction and transfer. Haemolymph was extracted or re-injected into flies using NanojectII (Drummond). Transgene expression in donor flies was induced through the TARGET system by incubating approximately 9-day-old adult animals for 3 days at 29 °C. The maximum amount of haemolymph was then collected from both sides of the thorax of donor flies. Thin sterile glass capillaries were used with NanojectII apparatus that extracts the fly haemolymph primarily by capillary action, thus ensuring that only sterile and clean haemolymph containing circulating haemocytes was collected. Quantification (see below) shows that haemolymph collected from a single fly in this manner should contain about 85 haemocytes. The collected haemolymph was then quickly transferred into the recipients without exposing it to any external media. Two to three donor flies were used to transfer haemolymph into a single recipient fly of the same age (about 12 days old). Thus, in this way each recipient fly should receive at least 171–257

DOI: 10.1038/ncb3174

haemocytes (see below for calculations). Finally, the injected animals were allowed to recover overnight before Paraquat treatment or bacterial challenge for the described time period.

Haemocyte quantification. To quantify the number of haemocytes transferred from donor flies into the recipients, the maximum amount of haemolymph was collected from 5 wild-type hmlΔ::Gal4,UAS::GFP adult flies of a given age by the method described above, and dissolved into 100 µl of PBS. The total number of retrievable circulating GFP-positive haemocytes was then manually counted using a fluorescent microscope after platting the solution on glass slides. As the number of haemocytes extracted from the haemolymph of 12-day-old flies was significantly higher, animals of this age were always used in haemolymph transfer experiments. A separate method was used to compare the number of haemocytes in 3-day-old wild-type and HDD flies, where haemolymph collected from only one side of the thorax cuticle of 20 flies was collected in 10 µl PBS and haemocyte quantification was performed using a haemocytometer (LifeTechnologies) following the manufacturer's recommendations.

LacZ clone and MARCM clone induction. LacZ-marked clones were generated in hsFlp; X.15.29/X.15.33 flies[38] combined with the indicated genotypes. Flies (2–3 days old) were heat-shocked for 45 min at 37 °C and kept at room temperature for 7 days before being dissected. For MARCM clone induction[34], 2–3-day-old flies were heat-shocked for 45 min at 37 °C. The flies were either kept for 7 days at room temperature before dissection, or after 1 day subjected to bacterial infection for 24 h, and then kept for 3 days at room temperature before dissection.

Lifespan experiments. Lifespan experiments were performed following a previously described procedure[49]. Briefly, the hmlΔ::Gal4 driver was backcrossed 7 times with the wild-type flies ($y^1.w^1$). The resulting hmlΔ::Gal4/+ flies were then crossed either with wild-type (+/+) or UAS::Hid or UAS::DppRNAi (Bloomington Stock no. 33618; backcrossed four times with the wild-type) in separate bottles, each with at least 4 replicates. Progenies with different genotypes (as described in Supplementary Fig. 8F) from each bottle were then split into two and transferred to separate rearing cages, with a maximum population density of 100 animals per cage. Thus, survival of each cohort of about 50–100 flies in a certain cage could directly be compared with the sister fly group that had developed together as larvae in the same bottle but had a different genotype.

qRT-PCR analysis. Total RNA from intestines of 20 flies (Supplementary Figs 4A and 3E), or haemolymph of 50 flies (Supplementary Fig. 3J), or carcasses of 10 flies (Supplementary Fig. 3E) was extracted using Trizol (Invitrogen). cDNA was synthesized using an oligo-dT primer. Real-time PCR was performed on a Bio-Rad CFX96 detection system. Relative expression was normalized to Actin5C or Rp49 (RpL32). Primer sequences: Actin5C (F), 5′-CTCGCCACTTGCGTTTACAGT-3′; Actin5C (R), 5′-TCCATATCGTCCCAGTTGGTC-3′; Rp49 (F), 5′-TCCTACCAG CTTCAAGATGAC-3′; Rp49 (R), 5′-CACGTTGTGCACCAGGAACT-3′; Dpp (F), 5′-CAGCACGCCTTCGGCACCTT-3′; Dpp (R), 5′-GGCACTCGCTGTACGTGG ACTTCTC-3′; Upd3 (F), 5′-ACAAGGCCAGGATCACCACCAAT-3′; Upd3 (R), 5′-TGTACAGCAGGTTGGTCAGGTTGA-3′.

Statistical analyses. Animals of the same age and genotype that received diverse treatments in different experiments were indiscriminately selected in all experiments. No randomization was performed among differentially treated animals. To blind the investigators for allocation of treatments and the outcomes from experiments shown in Figs 1a–c, 3a–c,e, 5c and 7a,f and Supplementary Figs 3A, 4F, 6F and 8F genetically different cohorts were numerically or alphabetically marked at the time of parental crosses. Once a particular experiment was complete and required data had been collected blindly, the arbitrary marks were matched with parental genotypes to designate final results to actual genotypes of tested animals. For all other experiments, investigators were not blinded to allocation during experiment and outcome assessment. Sample size, mean, median, range, variation and number of replicates for individual experiments are described in the corresponding figure legends. No statistical method was used to predetermine sample size. Prism and MS Excel software were used for all statistical analyses.

66. Wang, L., Zeng, X., Ryoo, H. D. & Jasper, H. Integration of UPRER and oxidative stress signaling in the control of intestinal stem cell proliferation. *PLoS Genet.* **10,** e1004568 (2014).
67. Osterwalder, T., Yoon, K. S., White, B. H. & Keshishian, H. A conditional tissue-specific transgene expression system using inducible GAL4. *Proc. Natl Acad. Sci. USA* **98,** 12596–12601 (2001).
68. Ni, J. Q. *et al.* A genome-scale shRNA resource for transgenic RNAi in *Drosophila*. *Nat. Methods* **8,** 405–407 (2011).
69. McGuire, S. E., Mao, Z. & Davis, R. L. Spatiotemporal gene expression targeting with the TARGET and gene-switch systems in *Drosophila*. *Sci. STKE* **2004,** pl6 (2004).

nature cell biology

DOI: 10.1038/ncb3174

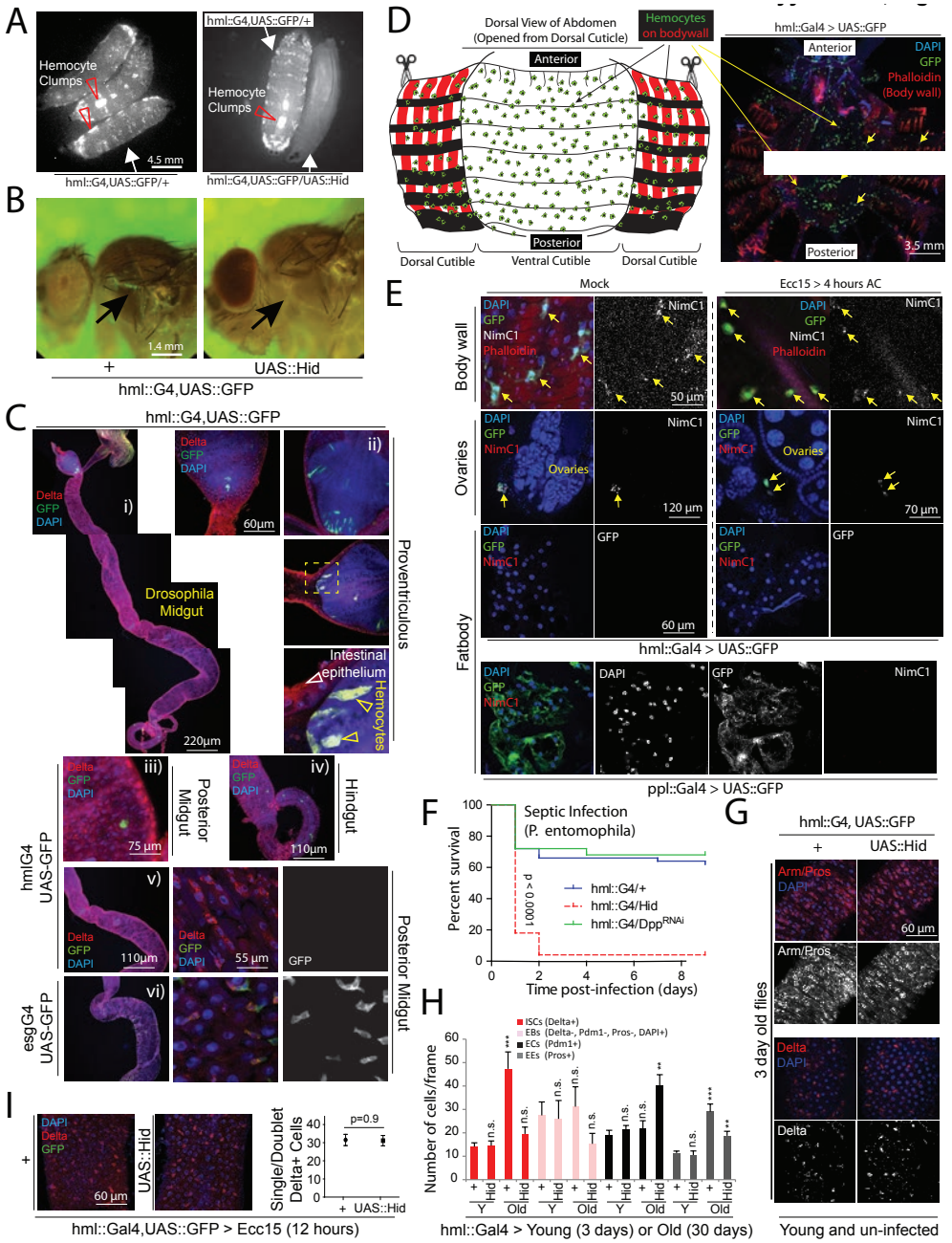

Supplementary Figure 1 Gut-associated hemocytes are required for ISC proliferation. (A,B) Hemocyte-ablated larvae (A) and adults (B) are shown, generated by expressing the pro-apoptotic gene *hid* specifically in hemocytes using *hmlΔ*::Gal4;UAS::GFP. GFP-positive hemocyte clumps are indicated by *red arrowheads*. (C) *hml* promoter expression in the whole adult gut is shown using hmlΔ::Gal4 (i). Variable number of extra-epithelial GFP-positive hemocytes can be detected in the proventriculous (ii; note that hemocytes (*yellow arrowheads*) are not part of the intestinal epithelium (*white arrowheads*), sometimes attached to the epithelial surface in midgut (iii), or hindgut regions (iv) but are not part of the epithelium that contains Delta-positive and esg::Gal4 expressing ISCs (v, vi). (D,E) *hmlΔ*::Gal4;UAS::GFP+ hemocytes attaching the abdominal body wall (D) also express the phagocyte marker NimC1 (E). Ovaries and fat body are *hmlΔ*::Gal4- and NimC1- (E). (F) Hemocyte-deficient flies rapidly succumb while both HDD and wild-type flies survive systemically disseminated *P. entomophila*. (G) Intestine in hemoless flies is normal in size and structure, and contain a normal distribution of cells (βCatenin/Armadillo labels cell boundaries and is highly expressed in ISC/EB nests; Prospero in enteroendocrine cells, and Delta in ISCs). (H) Intestinal cell composition. Absence of hemocytes does not change the composition of cells in the midgut of young animals. However, an increased number of Delta-positive ISCs observed in old wild-type animals is reduced in hemoless flies. (I) Representative images showing that intact Delta+ ISCs can be detected in the posterior midguts of hemocless flies at 12 hours post-Ecc15 infection. Error bars indicate s.e.m. (H: n=10 and I: n=8 flies tested in a single experiment, p values taken from Student Ttest; and experiment was replicated 3 (in panel H) and 2 (in panel I) times. Survival curves shown in panel F were compared using Prism software (n=20 flies tested in one experiment, p values were taken from LogRank test, and experiment was repeated 3 times. Single representative images from 10 flies used in a single experiment are shown in panels A-E and G while experiment was reproduced 3 (in panels A,B,D-I and G) or 2 (in panel C) times. n.s. = non-significant, **p<0.01, ***p<0.001.

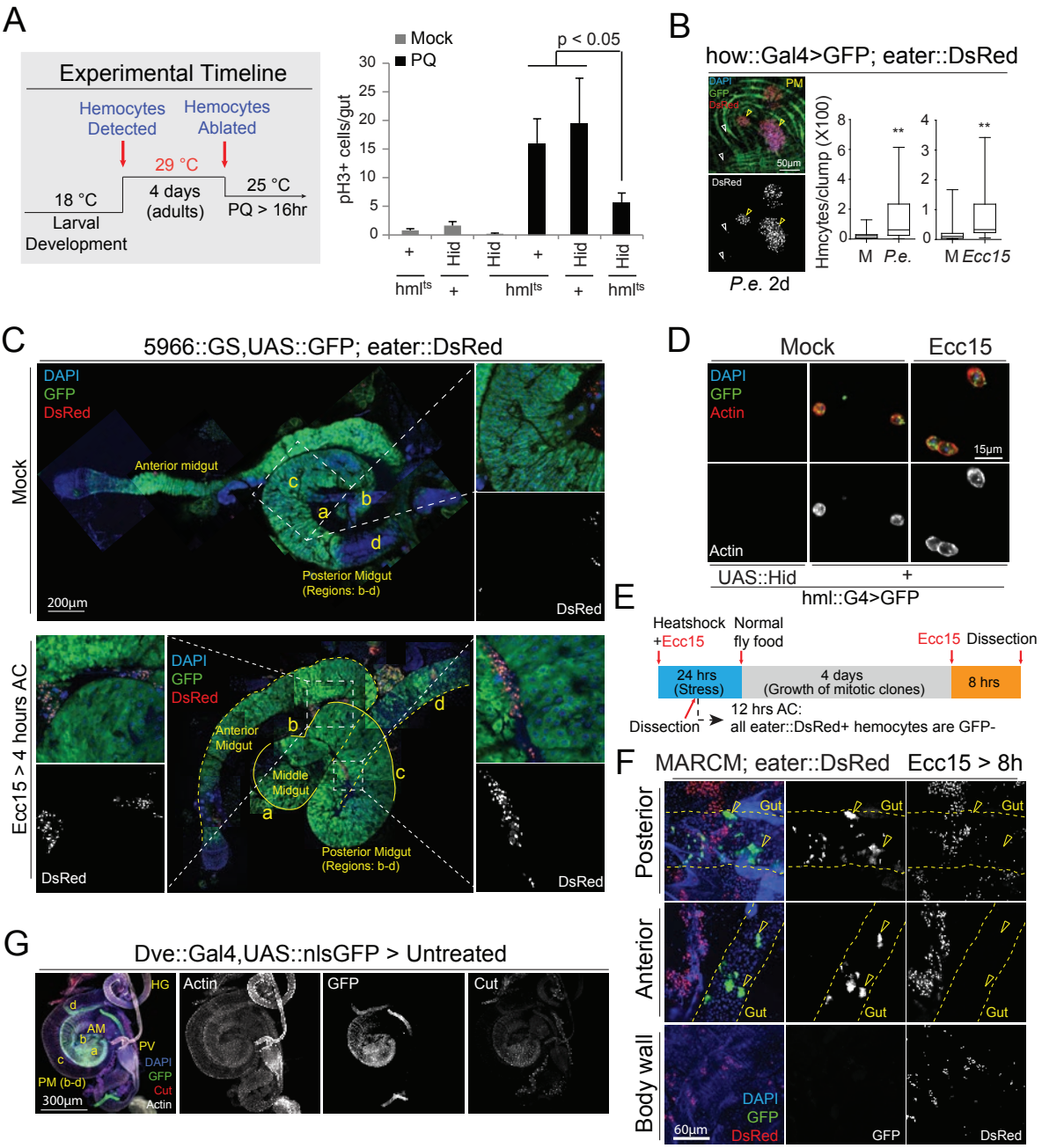

Supplementary Figure 2 Hemocytes recruited to stressed guts represent a post mitotic hematopoietic population. (A) PQ-induced ISC proliferation when hemocytes were ablated at 2 days of age by expressing *hid* with *hmlΔ*::Gal4, UAS::GFP, tub::Gal80^{ts} for 4 days. Hemocyte ablation was monitored visually in intact adults (not shown). Flies were exposed to Paraquat (PQ in 5% sucrose) or Mock (5% sucrose) for 16 hours at 25 ºC. (B) Hemocytes attached to the external surface of midgut regions a and b (identified by how::Gal4,UAS::GFP; see Fig.2B), following 2 days of *P. entomophila* infection. Quantification of eater::DsRed+ cells per gut-associated hemocyte clump 2 days after *P. entomophila* or 4 hours after *Ecc15* infection; M: mock. (C) 5966::GS,UAS::GFP flies co-expressing eater::DsRed fed RU846 food for 2 days followed by oral infection with *Ecc15* for 4 hours. (D) Circulating hemocytes change their size and shape at 4 hours post-*Ecc15* infection. F-actin detected by Phalloidin (red). (E,F) MARCM competent flies co-expressing eater::DsRed (see Supplementary Table 1 for exact genotype) subjected to *Ecc15* challenge and simultaneously heat shocked. No GFP+ hemocytes were observed at 12 hours after *Ecc15* infection (Analysis I) or at 5 days post heat shock (with or without a second *Ecc15* challenge: Analysis II) in any tissue (E; and not shown). GFP+ ISC-derived clones can be observed within the intestinal epithelium (F). (G) Expression pattern of dve::Gal4,UAS::GFP in midgut. PV: proventriculus, AM: anterior midgut, PM (b-d): posterior midgut regions b-d, HG: hindgut; Cut marks Copper Cells in middle midgut (compare [18]), here designated as region 'a' of the midgut. Error bars indicate either s.e.m. (A: n=12 flies) or range (B: for mock/P.e.: n=22 flies, for mock/Ecc15: n=32 flies; where boxes show 25-75% percentile and horizontal bar within each box is population median) calculated from single experiment. p values from Student's Ttest, reproduced in 3 independent experiments. Single representative image from 15 flies is shown in B-D,F and G, experiment was repeated 3 (in panels B,C and G) and 2 (in panel D-F) times. ***p<0.001.

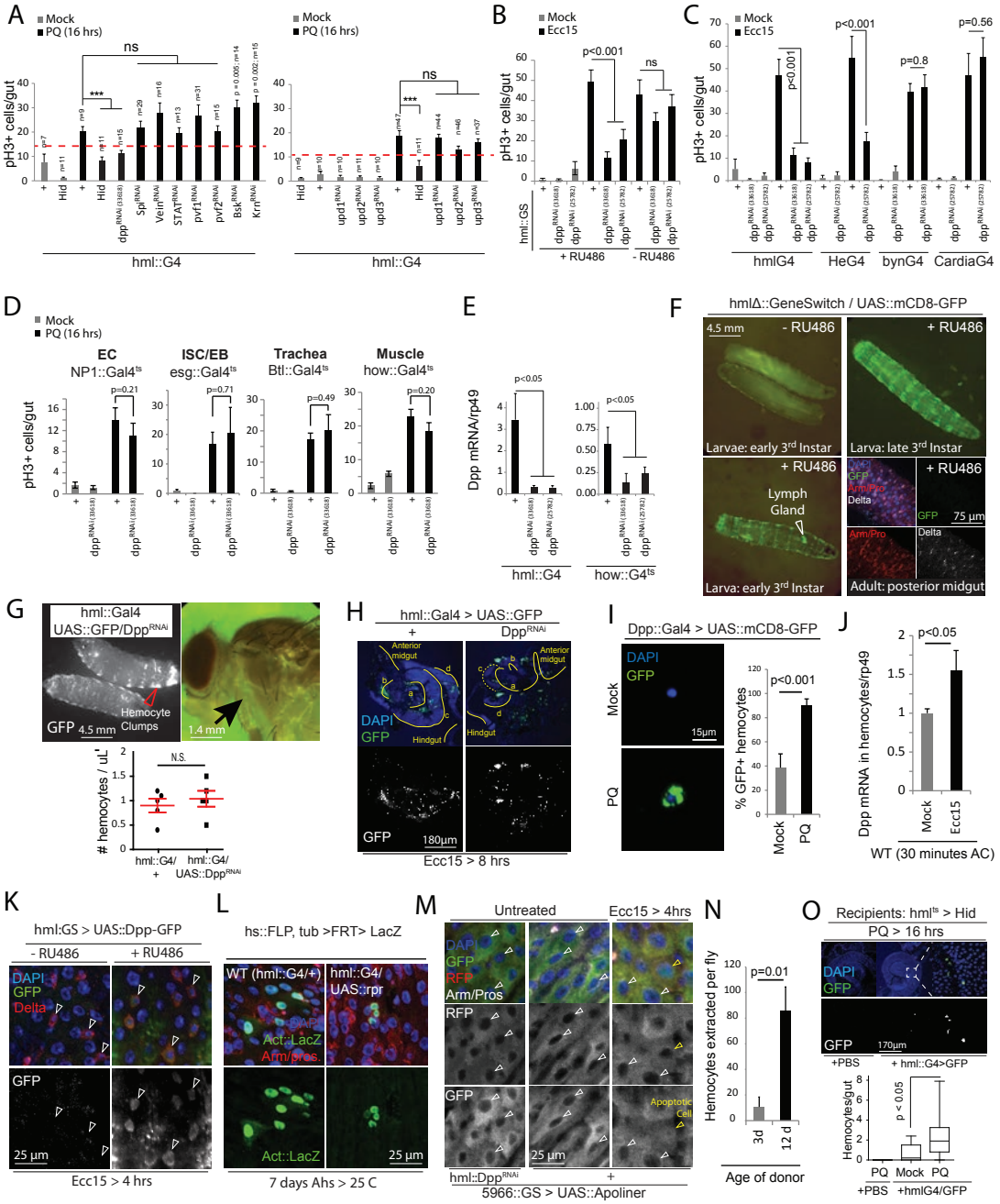

Supplementary Figure 3 Hemocyte-derive Dpp is required for ISC proliferation. (A) Hemocyte-specific RNAi screen assessing ISC activity upon PQ treatment. (B) Knockdown of Dpp using hmlΔ::GS. RU486 fed for 2 days followed by 8 hours *Ecc15* challenge. (C) ISC proliferation at 8 hours post-*Ecc15* in animals with knockdown of Dpp in hemocytes (hmlΔ::G4 and He::Gal4), hindgut (byn::Gal4) or proventriculus (Cardia::Gal4). (D) ISC proliferation upon Paraquat (PQ) feeding after Dpp knock down in ECs (NP1::Gal4), ISCs and EBs (esg::Gal4), trachea (Btl::Gal4) or visceral muscle (how::Gal4). (E) qRT-PCR to assess effectiveness of Dpp^{RNAi} lines in 10-15 day old adult carcass (containing hemocytes) using hmlΔ::Gal4, or in whole guts when using how::$G4^{ts}$ (29ºC 48 hours). (F) RU486-sensitive expression of UAS::mCD8-GFP in hemocytes and lymph gland of hmlΔ::GS larvae (no expression in adult gut epithelium). (G) GFP-positive, Dpp-deficient hemocytes in larvae and adults. Circulating hemocytes in adult hemolymph collected by Nanoinject II and counted using hemocytometer. (H) Dpp-deficient hemocytes attach to the intestinal epithelium during *Ecc15* challenge. (I) Percentage of GFP-positive hemocytes 16 hours post-PQ treatment in Dpp::Gal4,UAS::GFP flies. (J) Dpp transcript in hemocytes upon infection with *Ecc15* (30min after challenge). (K) Dpp-GFP from hemocytes (2 day feeding RU486) accumulates on ISCs (4 hours *Ecc15*). (L) Clones generated by FRT-mediated reconstitution of split actin::LacZ in wild-type or hemoless (hml::Gal4, UAS::Rpr) backgrounds. (M) Assessment of apoptosis by Apoliner (UAS::mcd8RFP::nlsGFP) expressed in ISC progeny (5966::GS). No apoptotic cells (nuclear GFP) are observed in hml::Dpp^{RNAi} flies. Apoptotic ECs can be observed during *Ecc15* infection. (N) Number of hemocytes retrieved from hemolymph at indicated ages. (O) PQ-induced recruitment of transplanted hemocytes to the gut of hemoless flies (donor: *hmlΔ*::Gal4,UAS::GFP). Error bars indicate s.e.m. (A: n's are indicated, composite of two (first graph) or three (second graph) experiments; B,E: n=10; G: n=5 (each sample represents a cohort of 20 flies); C,D: n=10; I,J: n=10; N: n=7) or range (O: n=9; boxes: 25-75% percentile. horizontal bar median value), Student T-test. All experiments, except A, replicated three times independently. Representative image (n=9) in F-I and K-M.; experiment repeated 3 times. n.s. = non-significant, ***p<0.001.

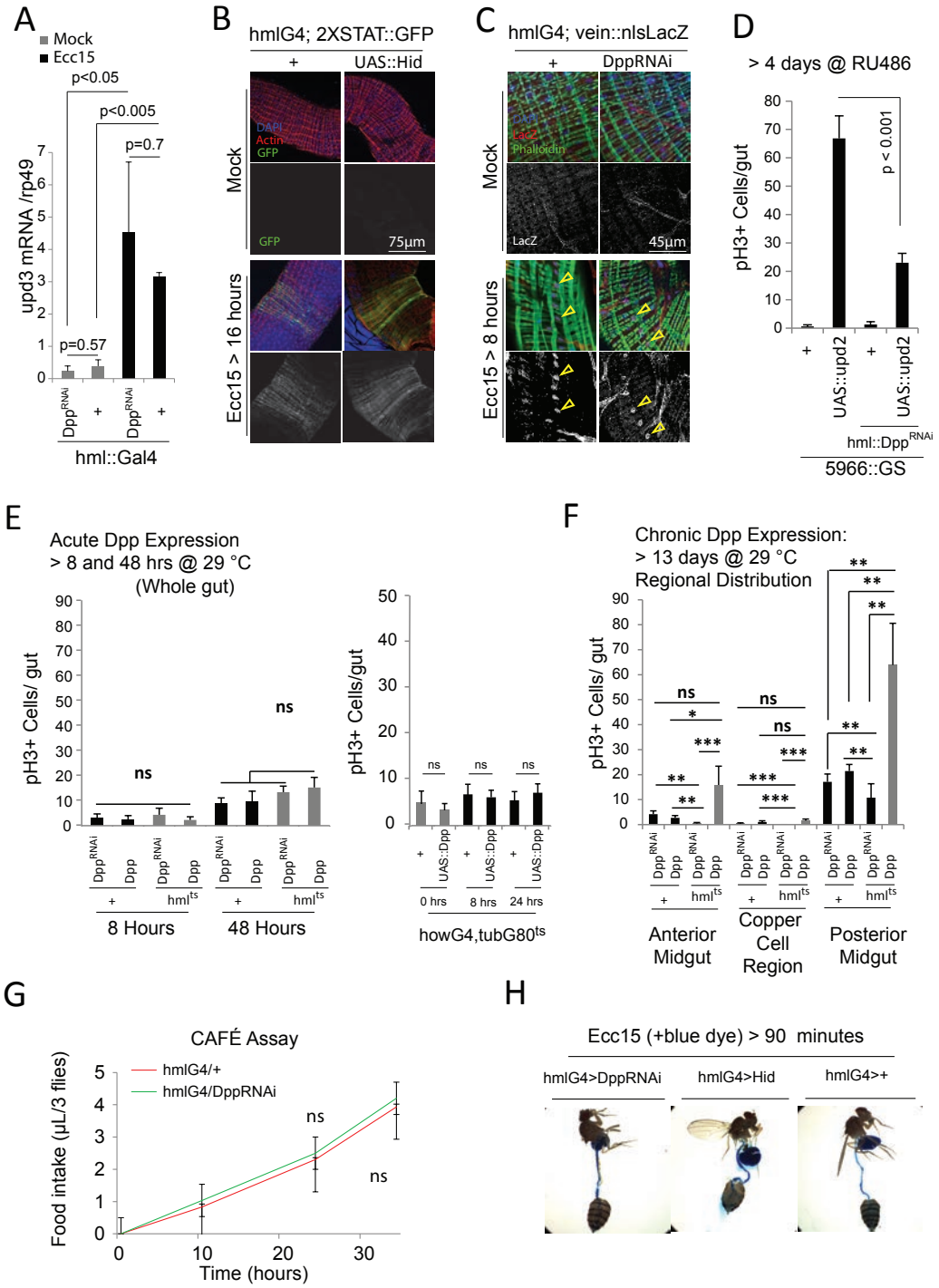

Supplementary Figure 4: Hemocyte-derived Dpp requires Jak/Stat and EGFR pathways to induce proliferation. (A-C) Transcription of Jak/Stat pathway activating ligand upd3 (A), expression of Jak/Stat activity reporter STAT::GFP (B), and EGFR ligand reporter Vein::LacZ (C: *arrowheads*) are normally induced in the intestine of HDD (A,C) and hemoless (B) flies during Ecc15 infection. (D) ISC proliferation induced upon upd2 overexpression in ECs is significantly reduced when Dpp expression is simultaneously blocked in hemocytes using an hmlΔ-Dpp^{RNAi} lines that does not use Gal4/UAS system (see methods). (E,F) Expression of UAS::Dpp was induced in adult hemocytes under the control of hmlΔ::Gal4 driver (which co-expressed tub-Gal80ts) by shifting 3 days old adult flies from 18 °C to 29 °C for indicated time intervals. Short-term expression of hemocyte-derived Dpp (i.e. for 8 or 48 hours) did not induce mitotic response in ISCs (E), while higher ISC proliferation was observed upon a long-term expression of Dpp in hemocytes for 13 days period. Over-expression of Dpp in visceral muscle (How::Gal4) for 8 or 24 hours does also not induce ISC proliferation. Error bars indicate s.e.m. (n>7), p values from Student Ttest. (G,H) HDD flies exhibit normal feeding in the absence of stress (assessed by the CAFÉ assay; G) or when fed on Ecc15 infection solution mixed with a blue dye for 90 minutes, following 2 hours of starvation period (H; note that digestive tracts are full of blue dye). Error bars indicate s.e.m. (A: n=4; D-F: n=10; and G: n=9 flies were used in one experiment), p values from Student Ttest, while results were reproduced in 2 independent experiments. Panels B (n>9), C (n>8) and H (n>15) show single representative images from 9 (panel B), 8 (panel C) and 15 (H) flies, and each experiment was replicated twice. n.s. = non-significant, *p<0.05, **p<0.01, ***p<0.001.

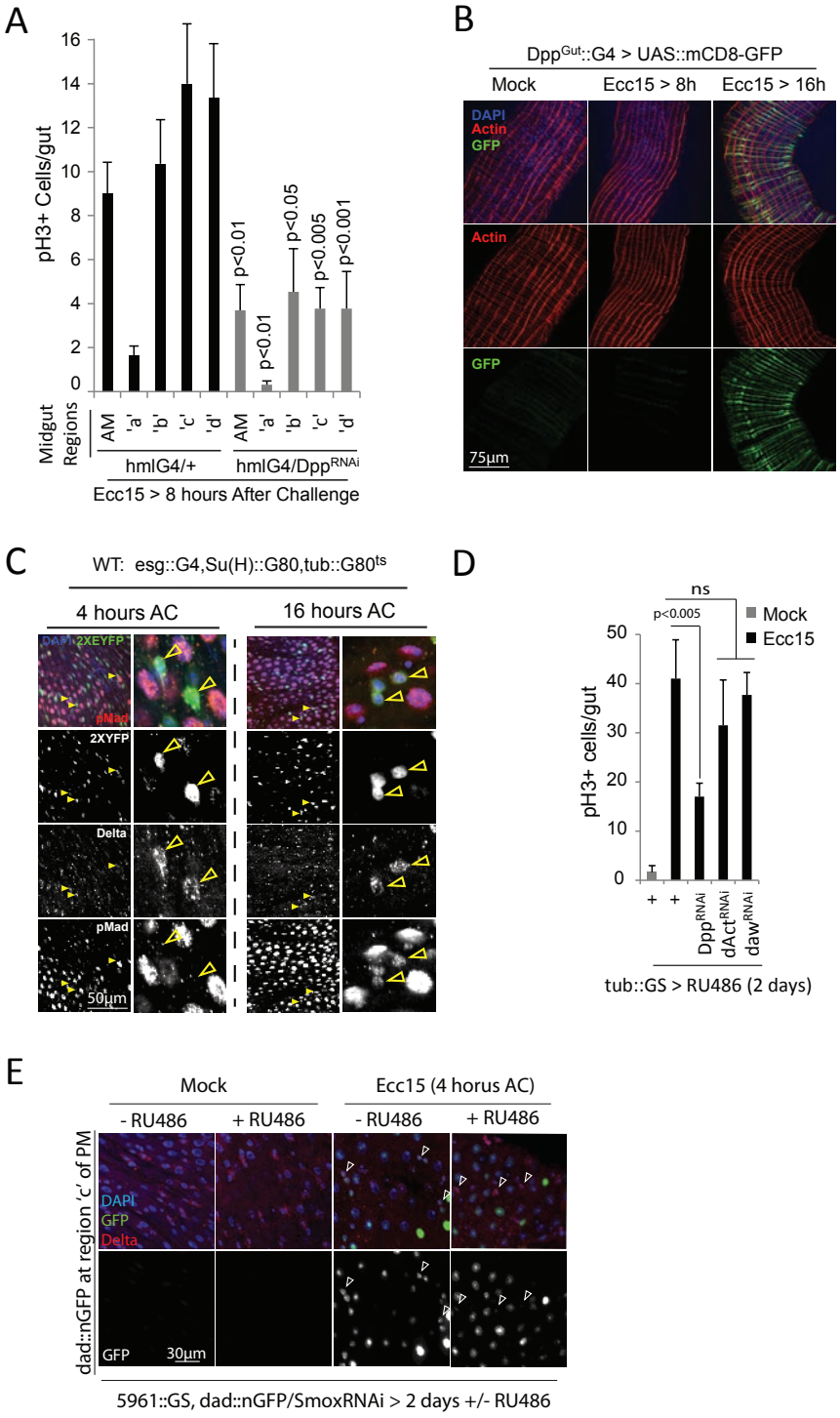

Supplementary Figure 5 Hemocyte-derived Dpp induces ISC proliferation in all gut regions, independent of Mad. (A) Reduced ISC proliferative response in HDD flies upon Ecc15 infection is observed in the entire length of the *Drosophila* adult midgut: anterior midgut (AM), Copper Cell Region (region 'a') and posterior midgut (regions 'b-d'). (B) Induction of local Dpp expression in the visceral muscle at region 'c' is observed only after 16 hour post-Ecc15 infection. (C) Mad is not phosphorylated in ISCs of region 'c' of the PM 4 hours post Ecc15 infection, but phosphorylation can be detected at 16 hours after challenge (AC): *arrowheads*. Delta as well as YFP-positive cells are ISCs. (D) Ubiquitous knockdown of Dpp, but not of dActivin or dawdle, using Mifepristone (RU486) drug sensitive ubiquitously expressed driver tub-GS decreases ISC proliferative response 4 hours post-Ecc15 challenge. (E) Knock down of Smox using ISC-specific 5961::GS significantly reduces the expression of dad::nGFP specifically in ISCs, but not in other intestinal cells, in region c of the posterior midgut following 4 hours of *Ecc15* challenge (compare to Fig.4E). Error bars indicate s.e.m. (A: n=10 and D: n=7 flies from one experiment), p values taken from Student Ttest, while each experiment was repeated 3 times. One representative image is shown from 13 (in panel B), 7 (in panel C) and 10 (panel F) flies used in a single experiment, while each experiment was repeated twice (B) or three times (C,F). n.s. = non-significant.

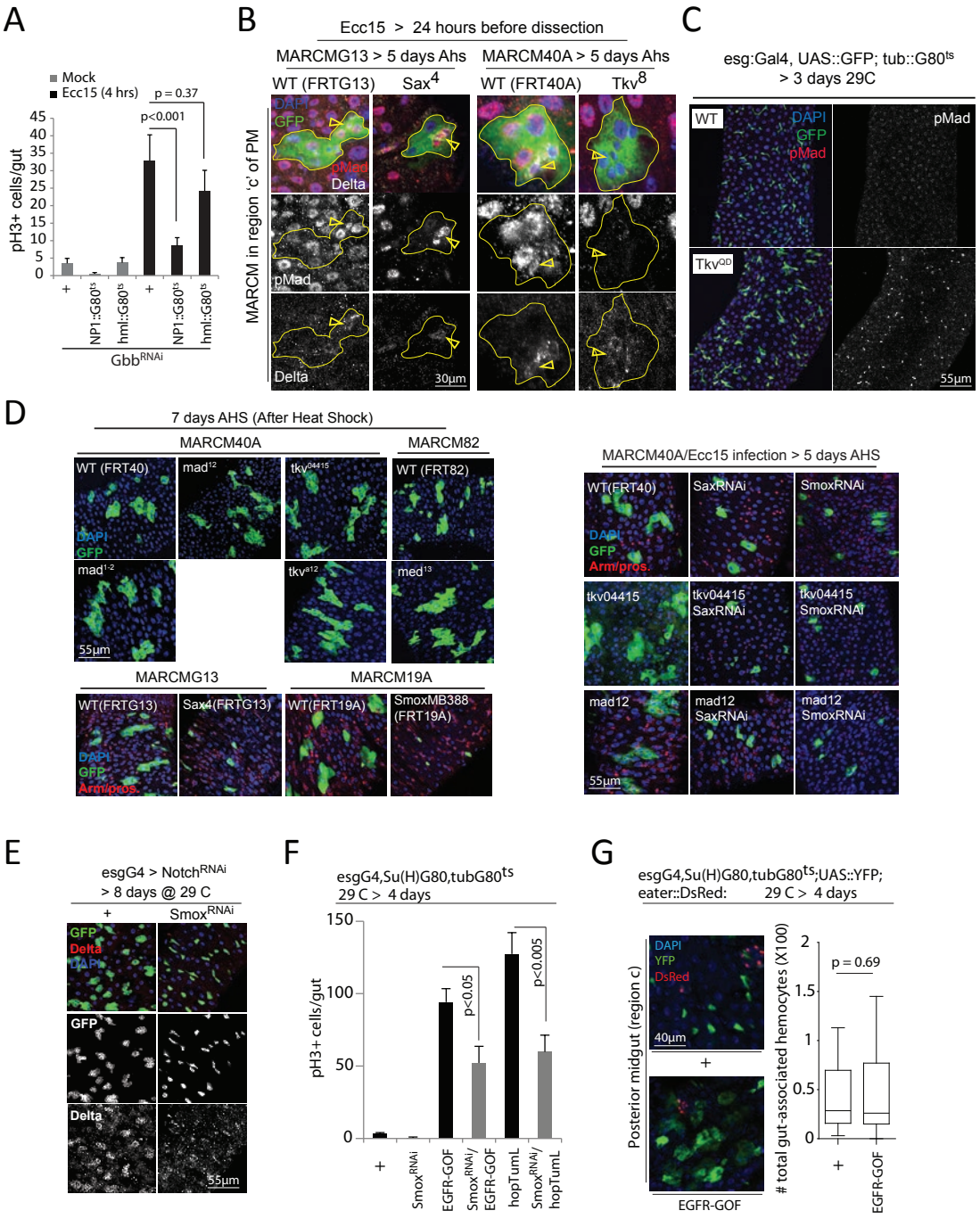

Supplementary Figure 6 Hemocyte-derived Dpp signals through Sax/Smox to induce ISC proliferation. (A) ISC proliferation at 4 hours of Ecc15 challenge. Gbb is knocked in adults in ECs (NP1::Gal4^{ts}) or hemocytes (hmlΔ::Gal4^{ts}). (B) Mad phosphorylation is absent in Tkv-, but not Sax-, mutant ISCs in MARCM clones in region 'c' of PM 24 hours post-Ecc15 challenge (*arrowheads*). (C) Over-expression of a constitutively active Tkv^{QD} in ISCs at region 'c' is sufficient to phosphorylate Mad in the absence of injury. (D) Representative images showing MARCM clones generated under normal conditions by mad^{12}, mad$^{1-2}$, tkv^{04415}, Tkv^{a12}, med^{13}, Sax^{4} and Smox^{MB388} mutant ISCs, and following *Ecc15* oral challenge by tkv^{04415} and mad^{12} mutant ISCs alone combined with ISC-specific Sax or Smox knockdown. (E) Smox knock down in ISCs suppresses the growth of ISC tumors in Notch loss-of-function conditions, which are formed by the accumulation of symmetrically dividing Delta-positive ISCs, a phenotype observed when Notch^{RNAi} is expressed under the control of ISC/EB specific driver esg::Gal4 [7,8]. (F) ISC over-proliferation induced by expressing EGFR-gain-of-function (EGFR-GOF) or constitutively active Hop (Hop^{TumL}) is rescued by simultaneous Smox knockdown. (G) Number of gut-associated eater::DsRed+ hemocytes does not increase upon EGFR-GOF over-expression. Error bars indicate either s.e.m. (A: n=14 and F: n=10 flies) or range (G: n=7 flies; where boxes show 25-75% percentile and horizontal bar within each box is population median) from one experiment, p values from Student Ttest; while each experiment was repeated twice. One representative image from 7 (panels B,C and G) and 10 (panel E) flies used in a single experiment is shown, while experiment was repeated 3 (panels B,C,E) or 2 (panel G) times. Panel D shows one representative images for each data set quantified in Fig. 5D,E (see legends of Fig.5D,E for n, p values and repetitions).

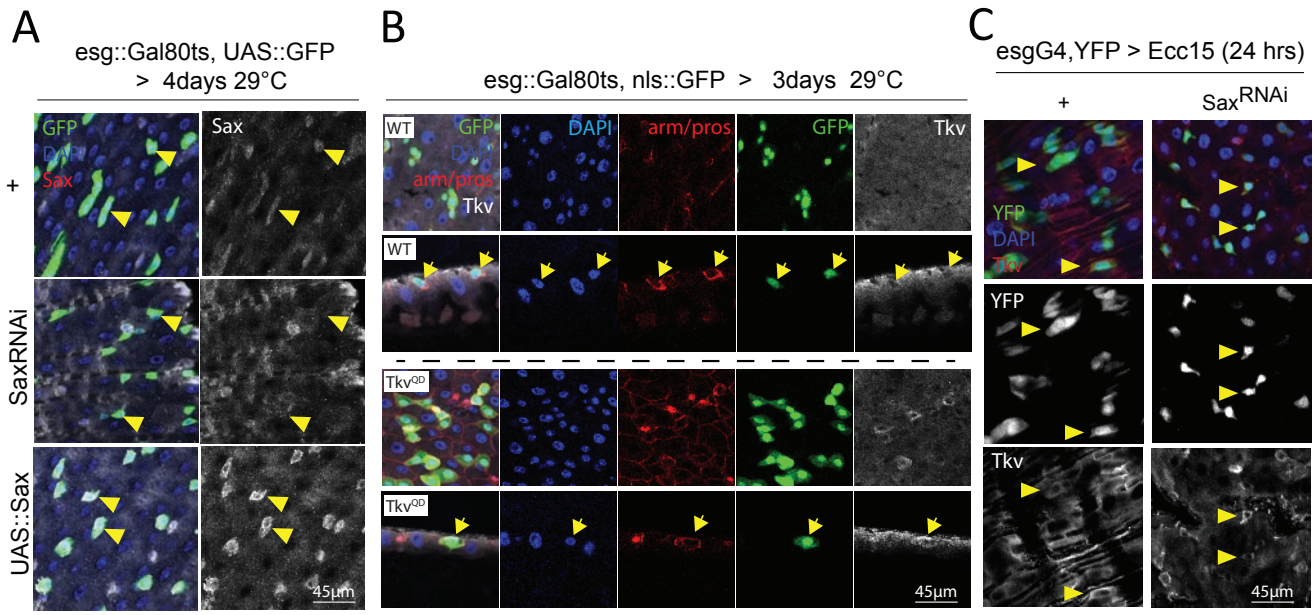

Supplementary Figure 7 Sax does not induce Tkv expression. (A) Sax detection in ISCs is lost upon RNAi knockdown using ISC/EB specific driver esg-Gal4, while an excessive staining is observed upon Sax overexpression within these cells (*arrowheads*), thus validating the specificity of the antibody used in this study. (B) Low expression of Tkv is detected in ISCs during basal conditions. Tkv^{QD}, when over-expressed in ISCs and EBs under the control of esg-Gal4, can be readily detected in these cells (*arrows*), confirming the specificity of the antibody used. (C) Sax knockdown in ISCs does not prevent late Tkv induction in ISCs following Ecc15 challenge (*arrowheads*). One representative image from 7 flies used in single experiment is shown in all panels, while each experiment was repeated twice.

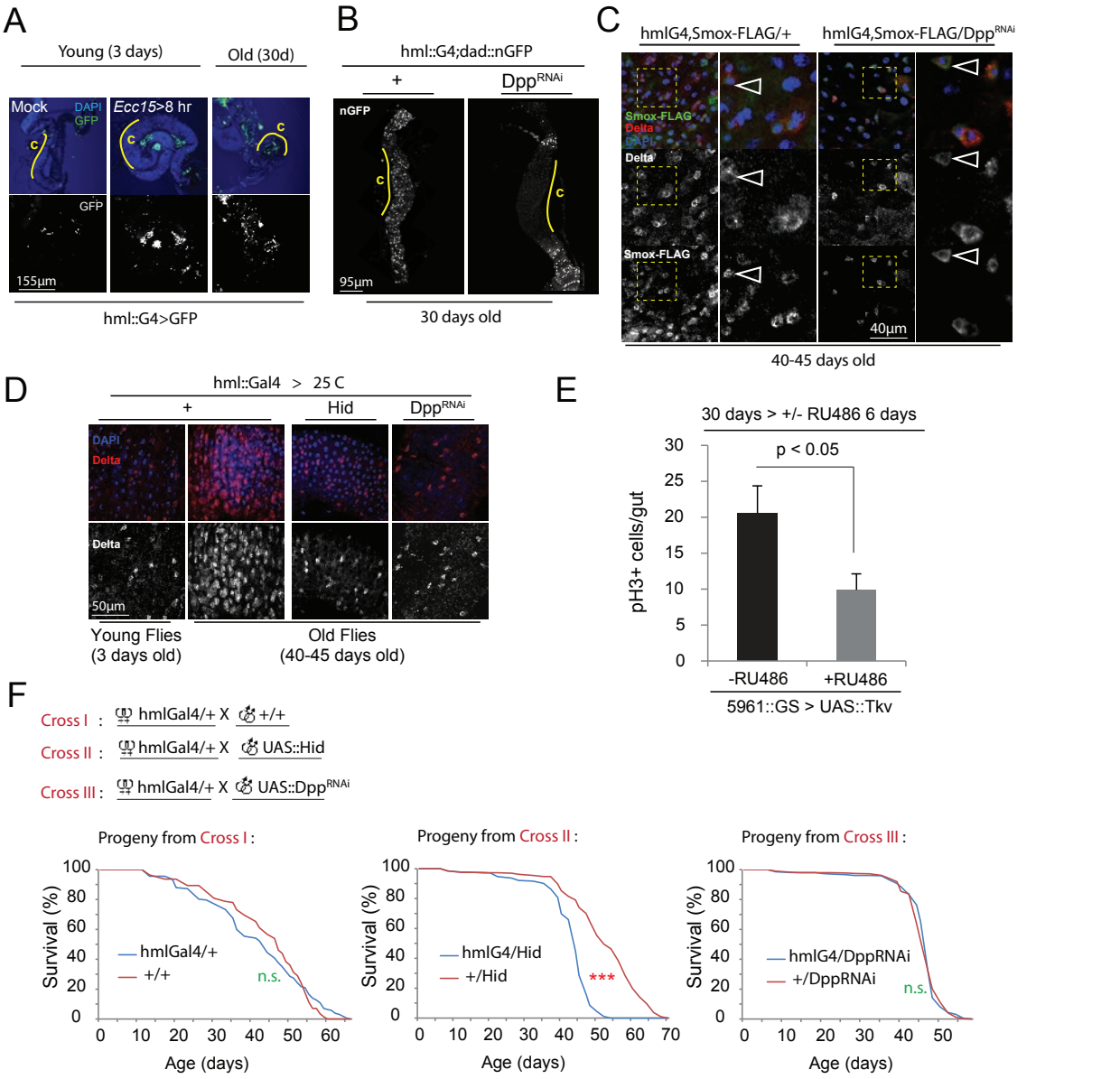

Supplementary Figure 8 Hemocyte-derived Dpp promotes intestinal dysplasia by inducing Smox nuclear localization. (A) Large numbers of hmlΔ::Gal4,UAS::GFP+ hemocytes (both as single cells or clumps) can be found attached to the intestine of young flies 8 hours after *Ecc15* challenge as well as in 30 day old untreated flies. (B-D) Images show hemocyte-derived Dpp dependent activation of BMP signaling pathway activation (note dad::nGFP reporter activity) in region c of posterior midgut (B), Smox nuclear localization (C) and development of intestinal dysplasia (D; note accumulation of Delta-positive cells). (E) Aged related overactivation of ISC proliferation, identified by the frequency of phospho histone H3+ (pH3+) cells per gut, is significantly reduced when 24 days old 5961::GS flies co-expressing UAS::Tkv transgene were shifted to RU846 drug containing food before observation at 30 days of age, thus, indicating that a relatively acute overexpression (for 6 days) of wild-type Tkv construct in ISCs can inhibit over activation of ISCs in aging animals. (F) Results from lifespan experiments are showing that where hemoless are significantly short-live, HDD flies live as long as their wild-type counter parts. Each survival curve represents a composite of total number of animals of a particular genotype tested (also see methods: *lifespan experiments*). Error bars indicate s.e.m. (E: n=14 flies used in one experiment), p values taken from Student Ttest, while results were reproduced twice. One representative image from 15 (panel A) or 7 (panels B-D) flies used in one experiment is shown, and each experiment was repeated two times.

					ChiSquare		p Value	
	Genotypes of tested progeny	n	Median Survival	Percentage Change	Log Rank	Wilcoxon	Log Rank	Wilcoxon
Progeny from Cross I	hmlG4/+	157	44	6.80%	0.1	2.07	0.75	0.15
	+/+	141	47					
Progeny from Cross II	hmlG4/Hid	400	44	18.20%	323.3	222.8	<0.0001	<0.0001
	+/Hid	400	52					
Progeny from Cross III	hmlG4/DppRNAi	409	47	0%	0.89	2.47	0.34	0.12
	+/DppRNAi	393	47					

Supplementary Table 1 List of genotypes
Genotypes for all fly lines used in this study are enlisted for the corresponding figures where the respective data have been shown.

Supplementary Table 2 Statistics for lifespan experiments.
Sample size, median survival and statistical tests used to analyze statistically significant differences in the lifespan of flies with various genotypes are summarized in this table.

Reference Figures	*Genotypes used*
Figure 1:	hmt_G4/+: hmtΔ::Gal4,UAS::GFP/+ hmt::G4/UAS::Hid: hmtΔ::Gal4,UAS::GFP/UAS::Hid hmtGS>mCherryVkg::GFP: hmtΔ::GeneSwitch,UAS::mcd8-Cherry::Vkg-GFP eater::DsRed
Figure 2:	dveGal4,UAS::nlsGFP, eaterDsRed howGal4,UAS::nlsGFP, eaterDsRed
Figure 3:	hmt::G4*: hmtΔ::Gal4,UAS::GFP; tub::Gal80ts hmt::GS.: hmtΔ::GeneSwitch UAS::DopRNAi (Bloomington Stock Number 33618) UAS::Dpp Oregon-R UAS::reaper UAS::Hid hsFLP::tub> FRT > LacZ::hmt::G4/+ : hsFLP; X:15.33/X15.29;hmtΔ::Gal4,UAS::GFP hsFLP::tub> FRT > LacZ::hmt::G4/Dpp^{blue} : hsFLP; X:15.33/X15.29;hmtΔ::Gal4,UAS::GFP/UAS::Dpp^{blue} hmt::GeneSwitch::UAS::mcd8::Cherry::UAS::Dpp::GFP: hmtG4::UAS::GFP : hmtΔ::Gal4,UAS::GFP;tub::Gal80ts hmtDP::UAS::GFP;UAS::Dpp::GFP : hmtΔ::Gal4,UAS::GFP;tub::Gal80ts/UAS::Dpp-GFP
Figure 4:	hmt::G4: hmtΔ::Gal4,UAS::GFP hmt::G4:Hid: hmtΔ::Gal4,UAS::GFP/UAS::Hid hmt::G4/Dpp^{blue}: hmtΔ::Gal4,UAS::GFP/UAS::Dpp^{blue} hmt::GS.: hmtΔ::GeneSwitch hmt::GS/ Dpp^{blue}: hmtΔ::GeneSwitch, /UAS::Dpp^{blue}
Figure 5:	WT: w1118, Smox-FLAG/+ hmt::G4/+;Dpp^{blue}/+ : hmtΔ::Gal4,UAS::GFP;tub::Gal80^{ts}/UAS::Dpp^{blue}; Smox-FLAG esg::G4>Sax^{exel} : esg::Gal4,tub::Gal80^{ts},UAS::Sax^{exel}; Smox-FLAG esgG4,Su(H)GBI:tubGBI^{ts} : esg::Gal4,Su(H)GBE::Gal80,UAS::2XEYFP;tub::Gal80^{ts} esgG4,Su(H)GBI:tubGBI^{ts}>Sax^{exel} : esg::Gal4,Su(H)GBE::Gal80,UAS::2XEYFP;tub::Gal80^{ts} ,UAS::Sax^{exel} esgG4,Su(H)GBI:tubGBI^{ts}>Smox^{exel} : esg::Gal4,Su(H)GBE::Gal80,UAS::2XEYFP;tub::Gal80^{ts} ,UAS::Smox^{exel} esgG4,Su(H)GBI:tubGBI^{ts}>Mad^{exel} : esg::Gal4,Su(H)GBE::Gal80,UAS::2XEYFP;tub::Gal80^{ts}, UAS::Mad^{exel} esgG4,Su(H)GBI:tubGBI^{ts}>tkv^{exel} : esg::Gal4,Su(H)GBE::Gal80,UAS::2XEYFP;tub::Gal80^{ts}, UAS::tkv^{exel} MARCM40A : hsFlp,UAS::GFP;FRT40, tub::Gal80/FRT40;tubGal4 MARCM40A tkv$^{8.2}$: hsFlp,UAS::GFP;FRT40,tub::Gal80/FRT40,tkv$^{8.2}$;tubGal4 MARCM40A_Smox^{EE1}: hsFlp,UAS::GFP;FRT40,tubGal80/FRT40;tubGal4/Smox^{exel} MARCM40A_Sax^{exel}: hsFlp,UAS::GFP;FRT40,tubGal80/FRT40;tubGal4/Sax^{exel} MARCM40A tkv$^{8.2}$; Smox^{EE1}: hsFlp,UAS::GFP;FRT40,tubGal80/FRT40,tkv$^{8.2}$;tubGal4/Smox^{exel} MARCM40A tkv$^{8.2}$; Sax^{exel}: hsFlp,UAS::GFP;FRT40,tubGal80/FRT40,tkv$^{8.2}$; tubGal4/Sax^{exel} MARCM40A Mad$^{1.36}$: hsFlp,UAS::GFP;FRT40,tubGal80/FRT40,Mad$^{1.36}$;tubGal4 MARCM40A Mad^{12}: hsFlp,UAS::GFP;FRT40,tubGal80/FRT40,Mad^{12};tubGal4 MARCM40A Mad^{12}; Smox^{exel}: hsFlp,UAS::GFP;FRT40,tubGal80/FRT40,Mad^{12};tubGal4/Smox^{exel} MARCM40A Mad^{12}; Sax^{exel}: hsFlp,UAS::GFP;FRT40,tubGal80/FRT40,Mad^{12};tubGal4/Sax^{exel} MARCM82 : hsFLP,UAS::GFP; tub::Gal4,FRT82,tubGal80/FRT82 MARCM82,med^{12}: hsFLP,UAS::GFP; tubGal4,FRT82,tubGal80/FRT82,med^{12} MARCM213 : hsFLP,UAS::GFP;FRT213,tubGal80/FRT213;tubGal4 MARCM213,sax^{4} : hsFLP,UAS::GFP;FRT213,tubGal80^{ts}/FRT13, sax^{4};tubGal4 MARCM19A : hsFLP;FRT19,tubGal80/FRT19;tubGal4,UAS::GFP MARCM19A smox^{EE1} : hsFLP;FRT19,tubGal80/FRT19, smox^{EE1};tubGal4,UAS::GFP esg::G4 UAS::mCD8GFP : esg::Gal4,UAS::mCD8-GFP esg::G4 2XEYFP : esgGal4,Su(H)GBE::Gal80,UAS::2XEYFP,tubGal80^{ts} esg::G4 UAS::mCD8GFP: esgGal4,UAS::mCD8-GFP esg::G4 2XEYFP : esgGal4,Su(H)GBE::Gal80,UAS::2XEYFP,tubGal80^{ts} w;Smox-FLAG
Figure 6:	WT (panel A): esg::Gal4,UAS::mcd8-GFP/+ WT (panel B and D): esgGal4,Su(H)GBE::Gal80,UAS::2XEYFP,tubGal80^{ts}/+ esgG4,Su(H)GBI:tubGBI^{ts}>UAS::Tkv: esgGal4,Su(H)GBE::Gal80,UAS::2XEYFP,tubGal80^{ts}/UAS::Tkv WT (panel C): w1118;Smox-FLAG/+
Figure 7:	hmtΔ::Gal4, UAS::GFP/+ hmtΔ::Gal4, UAS::GFP/ UAS::DppRNAi hmtΔ::Gal4, UAS::GFP/ UAS::Hid hmtΔ::Gal4, UAS::GFP/ 2XSTAT::GFP hmtΔ::Gal4, UAS::GFP, 2XSTAT::GFP/ UAS::DopRNAi hmtΔ::Gal4, UAS::GFP, 2XSTAT::GFP/ UAS::Hid hmtΔ::Gal4, UAS::GFP;Smox-FLAG/ hmtΔ::Gal4, UAS::GFP;Smox-FLAG/ UAS::DopRNAi
Supplementary Figure 1:	hmtΔ::Gal4,UAS::GFP UAS::Hid UAS::mCD8::GFP tep^{4}/+; hmtΔ::Gal4,UAS::GFP; tubGal80ts/+ hmt^{2}::Hid: hmtΔ/Gal4,UAS::GFP; tub::Gal80ts/UAS::Hid eater:DsRed
Supplementary Figure 2:	hmt^{2} hmtΔ/Gal4,UAS::GFP; tubGal80ts hmtΔ/Gal4,UAS::GFP; tubGal80ts/UAS::Hid hsp70-4>GFP: hmtΔ/Gal4,UAS::GFP 5966::GeneSwitch,UAS::GFP::eaterDsRed MARCM::eaterDsRed: hsFLPFRT19;tubGal80/FRT19/tubGal4,UAS::GFP; eaterDsRed Dve::Gal4,UAS::nlsGFP
Supplementary Figure 3:	hmtΔ/Gal4, UAS::GFP,UAS::Dop^{exel} (Bloomington Stock # 33618) hmtΔ/Gal4, UAS::GFP,UAS::Dop^{exel} (Bloomington Stock # 33618) hmtΔ/Gal4, UAS::GFP,tubGal80ts, UAS::Dpp hmtΔ/Gal4, UAS::GFP,UAS::SpitzRNAi hmtΔ/Gal4, UAS::GFP,UAS::VeinRNAi hmtΔ/Gal4, UAS::GFP,UAS::STATRNAi hmtΔ/Gal4, UAS::GFP,UAS::puRNAi hmtΔ/Gal4, UAS::GFP,UAS::puRNAi hmtΔ/Gal4, UAS::GFP,UAS::BskRNAi hmtΔ/Gal4, UAS::GFP,UAS::KrmRNAi hmtΔ/Gal4, UAS::GFP,UAS::upd1RNAi hmtΔ/Gal4, UAS::GFP,UAS::upd2RNAi hmtΔ/Gal4, UAS::GFP,UAS::upd3RNAi hmtΔ/GeneSwitch hmtΔ/GeneSwitch/ UAS::Dop^{exel} (Bloomington Stock # 33618) hmtΔ/GeneSwitch / UAS::Dop^{exel} (Bloomington Stock # 25782) how::Gal4,tubGal80ts/+ how::Gal4,tubGal80ts, UAS::DppRNAi tll::Gal4,tubGal80ts/+ tll::Gal4,tub-Gal80ts,UAS::DppRNAi NP1::Gal4,tubGal80ts/+ NP1::Gal4,tubGal80ts, UAS::DppRNAi esg::Gal4, UAS::GFP,tubGal80ts/+ esg::Gal4, UAS::GFP,tubGal80ts, UAS::DppRNAi hmt::Gal4, UAS::GFP/+ hmt::Gal4, UAS::GFP,UAS::DppRNAi # 1 (Bloomington Stock # 33618) hmt::Gal4, UAS::GFP,UAS::DppRNAi # 2 (Bloomington Stock # 25782) dpp/+Gal4/+ dpp/+Gal4/+,UAS::DppRNAi # 2 (Bloomington Stock # 25782) byn/Gal4/+ byn/Gal4, UAS::DppRNAi # 1 (Bloomington Stock # 33618) CarpGal4/++ CarpGal4, UAS::DppRNAi # 2 (Bloomington Stock # 25782) Dpp::G4/mCD8::GFP: Dpp::Gal4/UAS:mcd8-GFP hmtGeneSwitch::UAS::Dpp::GFP hsFLP::tub> FRT > LacZ::hmt::G4/+ : hsFLP; X:15.33/X15.29;hmtΔ::Gal4,UAS::GFP hsFLP::tub> FRT > LacZ::hmt::G4/UAS::rpr : hsFLP/UAS-Rpr; X:15.33/X15.29;hmtΔ::Gal4,UAS::GFP/UAS::Dpp^{blue} 5966::GeneSwitch,UAS::Apoliner 5966::GeneSwitch,UAS::Apoliner, hmtΔ::DppRNAi
Supplementary Figure 4:	WT: hmtΔ/Gal4,UAS::GFP/+ UAS::DopRNAi/+ UAS::Dpp/+ hmt/Gbe/UAS::Dpa : hmtΔ/Gal4,UAS::GFP; tubGal80ts, UAS::Dpp hmtGbe/UAS::DopRNAi : hmtΔ/Gal4,UAS::GFP; tubGal80ts, UAS::DppRNAi 2XSTAT::GFP, hmtΔ/Gal4 2XSTAT::GFP, hmtΔ/Gal4, UAS::Hid 5966::GeneSwitch/+ 5966::GeneSwitch/ UAS::upd2 5966::GeneSwitch/ UAS::upd2, hmtΔ::DopRNAi hmtΔ/Gal4, UAS::GFP, Vein::LacZ hmtΔ/Gal4, UAS::GFP, Vein::LacZ, UAS::DppRNAi +/UAS::DppRNAi +/UAS::Dpp hmtΔ/Gal4,UAS::GFP,tubGal80ts/UAS::DopRNAi hmtΔ/Gal4,UAS::GFP,tubGal80ts/UAS::Dpp hmtΔ/Gal4,UAS::GFP/+ hmtΔ/Gal4,UAS::GFP/UAS::DppRNAi hmtΔ/Gal4,UAS::GFP/UAS::Hid
Supplementary Figure 5:	hmtΔ/Gal4, UAS::GFP hmtΔ/Gal4, UAS::GFP,UAS::DopRNAi Dve^{nls}::G4/UAS:mCD8::GFP : Dve-Gal4 (Bloomington Stock # 45111)/UAS-mCD8-GFP WT : esg::Gal4,UAS::2XEYFP; Su(H)GBE::Gal80, tubGal80ts tubGeneSwitch tubGeneSwitch::UAS::DopRNAi tubGeneSwitch::UAS::dAdoIsinRNAi tubGeneSwitch::UAS::dawdleRNAi 5961::GeneSwitch, dad::nGFP;UAS::SmoxRNAi
Supplementary Figure 6:	NP1::G80^{ts}: NP1::Gal4, tub::Gal80ts NP1::G80^{ts}, GbtRNAi : NP1::Gal4, tubGal80ts; UAS::GbtRNAi (Bloomington Stock # 34898). MARCM40A : hsFlp,UAS::GFP;FRT40,tubGal80/FRT40;tubGal4 MARCM40A tkv$^{8.2}$: hsFlp,UAS::GFP;FRT40,tubGal80/FRT40,tkv$^{8.2}$;tubGal4 MARCM213 : hsFLP,UAS::GFP;FRT213,tubGal80/FRT213;tubGal4 MARCM213,sax^{4} : hsFLP,UAS::GFP;FRT213,tubGal80^{ts}/FRT13, sax^{4};tubGal4 esgGal4, UAS::GFP, tubGal80ts esgGal4, UAS::GFP, tubGal80ts, UAS::Tkv^{act} MARCM40A : hsFlp,UAS::GFP;FRT40,tubGal80/FRT40;tubGal4 MARCM40A tkv$^{8.2}$: hsFlp,UAS::GFP;FRT40,tubGal80/FRT40,tkv$^{8.2}$;tubGal4 MARCM40A_Smox^{EE1}: hsFlp,UAS::GFP;FRT40,tubGal80/FRT40;tubGal4/Smox^{exel} MARCM40A_Sax^{exel}: hsFlp,UAS::GFP;FRT40,tubGal80/FRT40;tubGal4/Sax^{exel} MARCM40A tkv$^{8.2}$; Smox^{EE1}: hsFlp,UAS::GFP;FRT40,tubGal80/FRT40,tkv$^{8.2}$;tubGal4/Smox^{exel} MARCM40A tkv$^{8.2}$; Sax^{exel}: hsFlp,UAS::GFP;FRT40,tubGal80/FRT40,tkv$^{8.2}$; tubGal4/Sax^{exel} MARCM40A Mad$^{1.36}$: hsFlp,UAS::GFP;FRT40,tubGal80/FRT40,Mad$^{1.36}$;tubGal4 MARCM40A Mad^{12}: hsFlp,UAS::GFP;FRT40,tubGal80/FRT40,Mad^{12};tubGal4 MARCM40A Mad^{12}; Smox^{exel}: hsFlp,UAS::GFP;FRT40,tub-Gal80/FRT40,Mad^{12};tubGal4/Smox^{exel} MARCM40A Mad^{12}; Sax^{exel}: hsFlp,UAS::GFP;FRT40,tubGal80/FRT40,Mad^{12};tubGal4/Sax^{exel} MARCM82 : hsFLP,UAS::GFP; tubGal4,FRT82,tubGal80/FRT82 MARCM82,med^{12}: hsFLP,UAS::GFP; tubGal4,FRT82,tubGal80/FRT82,med^{12} MARCM213 : hsFLP,UAS::GFP;FRT213,tubGal80/FRT213;tubGal4 MARCM213,sax^{4} : hsFLP,UAS::GFP;FRT213,tubGal80^{ts}/FRT13, sax^{4};tubGal4 MARCM19A : hsFLP;FRT19,tubGal80/FRT19;tubGal4,UAS::GFP MARCM19A smox^{EE1} : hsFLP;FRT19,tubGal80/FRT19, smox^{EE1};tubGal4,UAS::GFP 5961::GeneSwitch,dad::nGFP 5961::GeneSwitch,dad::nGFP; SmoxRNAi (Bloomington Stock # 26756) esgGal4, UAS-GFP, tubGal80ts, UAS::NotchRNAi esgGal4, UAS-GFP, tubGal80ts, UAS::NotchRNAi, UAS::SmoxRNAi (Bloomington Stock # 26756) esgGal4, UAS::2XEYFP, Su(H)GBE::Gal80, tubGal80ts/+ esgGal4, UAS::2XEYFP, Su(H)GBE::Gal80, tubGal80ts/UAS::SmoxRNAi (Bloomington Stock # 26756) esgGal4, UAS::2XEYFP, Su(H)GBE::Gal80, tubGal80ts/UAS::EGFR-DOF (constitutively active) esgGal4, UAS::2XEYFP, Su(H)GBE::Gal80, tubGal80ts/UAS::hopTumL (constitutively active) esgGal4, UAS::2XEYFP, Su(H)GBE::Gal80, tubGal80ts/UAS::EGFR-DOF (constitutively active)::eaterDsRed
Supplementary Figure 7:	esgGal4, UAS::GFP, tub::Gal80ts/+ esgGal4, UAS::GFP, tub::Gal80ts/UAS::SaxRNAi esgGal4, UAS::GFP, tub::Gal80ts/UAS::Sax esgGal4, UAS::nlsGFP, tubGal80ts/+ esgGal4, UAS::nlsGFP, tubGal80ts/UAS::Tkv^{act} esgGal4, UAS::2XEYFP, Su(H)GBE::Gal80, tubGal80ts/+ esgGal4, UAS::2XEYFP, Su(H)GBE::Gal80, tubGal80ts/UAS::SaxRNAi
Supplementary Figure 8:	hmtΔ/Gal4, UAS::GFP, dad::nlsGFP/+ hmtΔ/Gal4, UAS::GFP, dad::nlsGFP/ UAS::DopRNAi hmtΔ/Gal4, UAS::GFP, dad::nlsGFP/ UAS::Hid hmtΔ/Gal4, UAS::GFP,Smox-FLAG/+ hmtΔ/Gal4, UAS::GFP,Smox-FLAG, UAS::DppRNAi hmtΔ/Gal4, UAS::GFP/+ hmtΔ/Gal4, UAS::GFP,UAS::DopRNAi hmtΔ/Gal4, UAS::GFP,UAS::Hid 5961/GeneSwitch, UAS::Tkv hmtΔ/Gal4/+ hmtΔ/Gal4/UAS::Hid hmtΔ/Gal4/UAS::DppRNAi